View metadata, citation and similar papers at core.ac.uk
brought to you by CORE
provided by ScholarBank@NUS

Automatic Microassembly System for Tissue Engineering - Assisted with Top-View and Force Control

MENG QINGNIAN

NATIONAL UNIVERSITY OF SINGAPORE

2007

Acknowledgements

First and foremost, I want to express my most sincere gratitude to my supervisors, Dr. TEO Chee Leong and Dr. Etienne BURDET, for their valuable supervision, constructive guidance, incisive insight and enthusiastic encouragement throughout my project.

I wish to specifically thank Mr. ZHAO Guoyong, my partner in this project, for his constant help in all aspects of this work.

I also express my appreciation to Dr. Franck Alexis CHOLLET and his group in the Micro Machine Centre (MMC) at Nanyang Technology University (NTU) for his kind guidance on the design and fabrication of the micro parts. I wish to thank Mr. MOHAMMED Ashraf for his help in the cleanroom work and his friendship.

I also would like to thank National University of Singapore for their financial support and research facilities. Without these supports, the study will not be possible. I am also grateful to the staff in the Control and Mechatronics Lab, for their assistance and kindness.

My gratitude is also extended to the colleagues and friends in our lab and NUS, Mr. ZHU Kunpeng, Mr. Du Tiehua, Mr. WANG Chen, Mr. WAN Jie, Mr. LU Zhe, Mr. ZHOU Longjiang, Ms. SUI Dan and many others, for their enlightening discussion, suggestions and friendship.

Finally, I owe my deepest thanks to my parents, my family, and my girlfriend, Ms. JI Yingying, for their unconditional and selfless encouragement, love and support.

Table of Contents

Summary

One of the main problems of present automatic microassembly techniques is the lack of the implementation of force control, especially the control of the assembly force or the insertion force. This thesis develops techniques for efficient z-axis microassembly based on force control of commercially available stages. These techniques arise from an application in tissue engineering.

Microassembly technique has shown much potential in facilitating tissue regeneration tasks. In this work, an automatic system is developed for building 3D tissue engineering scaffold by assembling microscopic building blocks. The idea is to coat the micro parts with specific and individual cells and bioagents, and then assemble them into 3D scaffold in biocompatible environment with certain desired spatial distributions.

3D cross-like micro part was designed and fabricated for the assembly task. Its overall dimension is $500\mu m \times 500\mu m \times 200\mu m$ with a through hole in the centre of $100\mu m$ in diameter, and the wall thickness is $60\mu m$. The parts were fabricated from SU8 using photolithography process. The structure allows assemble the parts only by pushing them down from above, and then the parts will stick together by friction.

The developed 5 DOF desktop workstation contains five micron precision micropositioning stages, one microscope and one force sensor integrated gripper. The prototype micro probe gripper was fabricated using electrochemical etching technique,

with a photolithography fabricated pushing shoulder for assembly, with a fine tip that matches the hole in the part for grasping. The force sensor was developed by attaching two semiconductor strain gauges to a specifically designed elastic element. A force-based admittance controller was implemented to the process for guiding the grasping and assembling process.

Experimental results show high efficiency and high yield of the system. With the admittance controller, the system is robust to the variation of the dimension of micro parts. And we note that apart from the assembly tasks, this automated workstation can be used in other applications such as manipulating biological cells or testing silicon chips.

List of Tables

List of Figures

Chapter 1

Introduction

1.1 BACKGROUND

Assembly is often required in macroscale product manufacturing in order to reduce the complexity and cost of the manufacturing process. Assembly makes it possible to build complex products from relatively simple parts and to integrate incompatible manufacturing processes. It also makes maintenance and replacement possible. The extension of assembly techniques into micro/meso-scale1 is driven by the development of modern design and manufacturing technologies in the pursuit of miniaturization and function integration. To miniaturize a product it is not sufficient to simply reduce its dimensions. A lot of new problems emerge, related to scaling effects, manufacturing problems and, of course, assembly problems. One of those problems has to do with the fact that, up to now, nearly all production techniques for microsystems have their origin in the microelectronics technology, and are essentially 2D processes.

In the last two decades, automatic microassembly has bloomed due to the demand of micro photonics devices, electro-mechanical systems, and bioengineering, etc, and the requirement is to improve productivity as well as the accuracy relative to manual assembly. One of the main problems of present automatic microassembly techniques is the

implementation of force control, especially of the assembly force or the insertion force. One solution is to use z-axis assembly, which can be found in some peg insertion tasks and usually requires 3 or 4 DOF, with 2 for the locating and one or two for grasping (Nakagaki H. et al, 1995), (Hara H. et al, 1997), (Bruzzone L.E. et al, 2002), etc. This thesis develops techniques for efficient z-axis microassembly based on force control, using commercially available stages.

These techniques arose from an application in tissue engineering. The loss or failure of an organ or tissue is one of the most frequent, devastating, and costly problems in health care, and transplantation surgery is always implemented to treat this disorder. Tissue engineering, implementing tissue regeneration by autogenous cell transplantation, is a new and promising technique, since it has the potential to provide the ideal autograft. This can avoid almost all the limitations of conventional transplantation, such as gene rejection, donor shortage, long-term survival problems, etc. (Langer, Vacanti, 1993). Most tissue engineering strategies for creating functional replacement tissues of organs rely on the application of temporary three-dimensional scaffolds to guide the proliferation and spread of seeded cells in vitro and in vivo (Zhang, 2005). For example, matrix-producing connective tissue cells or anchorage-dependent cells taken from a patient can be seeded onto a three-dimensional scaffold in vitro. The scaffold is made to the shape of the wound, should be covered by or immersed in culture liquid in advance. In this way, the cells will proliferate, migrate and differentiate into the tissue while secreting the extracellular matrix components required to create the tissue. In time the scaffold will degrade and be absorbed

by the growing cells as nutrition. Finally, the structure will function coordinately with the rest of the body without complications.

To achieve the successful regeneration of tissues and organs, which includes cell survival, signaling, growth, propagation and reorganization, as well as cell shape modeling, and gene expressions that relate to cell growth and the preservation of native phenotypes, there are certain requirements of the tissue engineering scaffolds' materials, macro- and microstructure properties, etc. as follows:

- *Material*: The scaffolds materials are confined to those that are non-mutagenic (not containing physical or chemical agent that changes the genetic information of an organism), non-antigenic (not producing substances that stimulate immune response), non-carcinogenic (not causing cancer), non-toxic and non-teratogenic (not leading to malformations) and possess high cell/tissue biocompatibility, and most importantly, should be biodegradable and bioresorbable (Leong et al, 2003).
- *Macrostructure*: The choice of the temporary three-dimensional scaffold is crucial to enable the cells to behave in the required manner to produce tissues and organs of the desired shape and size.
- *Porosity and pore interconnectivity*: The scaffold should be highly porous (exceeding 90%) in its surface and microstructure and have open-pore geometry, which will ensure healthy growth of the seeded cells as well as the use of bioreactors (Vacanti et al, 1988; Mikos et al, 1993).
- *Pore size*: The microenvironment for the generation of different tissue is quite diverse. Hence the pore size of the scaffold must be designed for the specific purpose. The

sizes usually vary from tens of to hundreds of microns (Robinson et al, 1995), (Yannas et al, 1989), (Kim et al, 1998).

- *Surface area and surface chemistry*: a large quantity of cells is needed to regenerate the tissue or organ function, and so the internal surface area should be maximized to hold those cells. And the surface chemistry, which is dependent on the material of the scaffold, is important for the growth of the cells (Healy et al, 1992), (McClary et al, 2000).
- *Mechanical properties*: The scaffold should have enough mechanical strength to guide the tissue regeneration, especially during the degrading period of the scaffold (Mikos et al, 1993).

Besides the previously listed pre-requisites for tissue regeneration scaffold, there are still requirements for scaffold fabrication techniques, such as process accuracy, consistency, repeatability, and etc.

Based on all these requirements, the major goal of bioresorbable 3-D scaffold fabrication is to achieve high levels of accurate control over their macro- and microstructural properties. A teleoperated scaffold microassembly system (Figure 1-1) based on manual operation has been implemented and evaluated, and the goal of this thesis is to automate the whole system by adding multisensory information of force and vision to it with concentration on the force part.

1.2 DEFINITION OF THE PROBLEMS

Previously, the assembly process was accomplished by an operator through teleoperating the workstation (Figure 1-1) on a PC. The operator can get the side views of the work space through two microscopes, and use the visual information to control the assembly process. The assembly task is to find the micro part for assembly on the wafer, move the gripper to the part and pick it up, move the gripper to the assembly area and find the position to put the part to assemble the structure. The manual assembly process has several disadvantages:

- *Time consuming*: Building a pyramid shape scaffold (Figure 1-1D) consisting of about 100 parts by an experienced operator using the system needs about one week, and a scaffold for practice use may consist of thousands of parts.
- *Low accuracy*: The gripper used previously (Figure 1-1C, D) can only grasp one branch of the part. This will lead to an unbalanced pushing force and cause the part to tilt. The whole process is controlled manually by a human operator, and this will also decrease the accuracy of the assembled scaffold due to the limitation of human.
- *Operator dependence*: An operator must be well trained before he or she can operate the system, as the micro parts and the tip of the gripper are both in hundreds of microns dimension and very fragile.

1.3 OBJECTIVES AND SCOPE OF THE STUDY

From the above listed disadvantages, it can be easily seen that most of the problems owing to the operator being involved in much of the process. A solution is to make the assembly process independent of the operator, which means to automate the whole process.

A

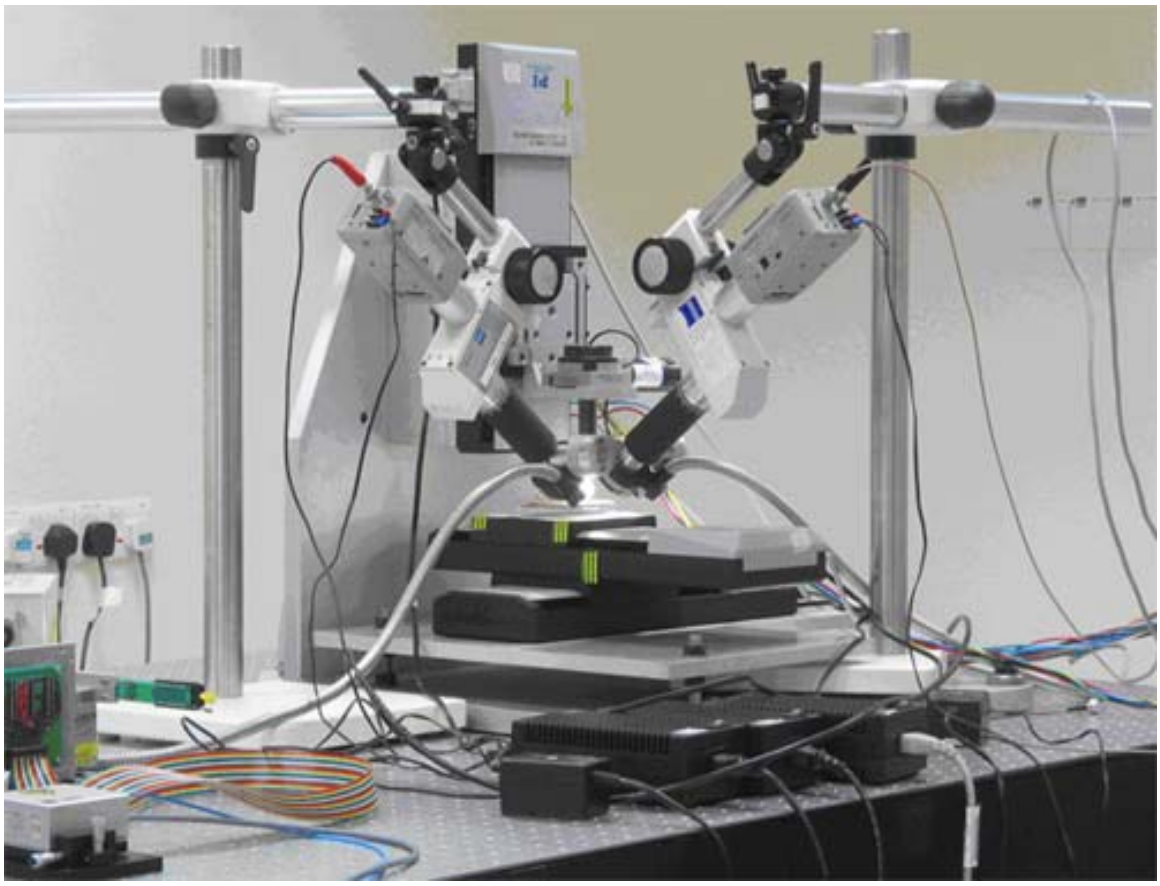

B

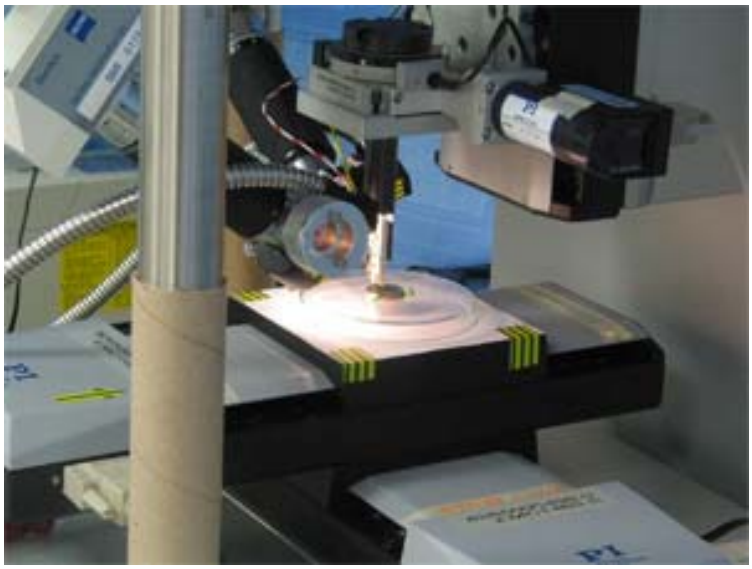

C

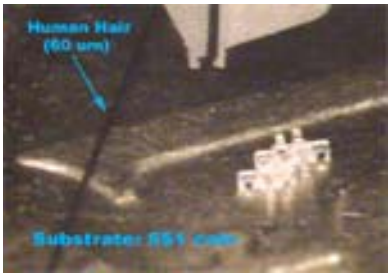

D

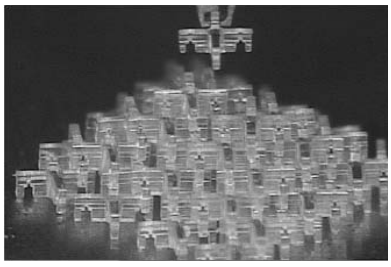

Figure1-1: (A) The scaffold assembly workstation previously used. (B) Amplification of the Gripping part of the previous workstation. (C) A small scaffold under the previous gripper compared with a human hair. (D) A large scaffold assembled (3x3x2mm).

Our goal is to develop a fast and high yield 3D microassembly which without damage the parts during assembly. Previous works has emphasized the role of visual control in microrobotics (Nelson et al, 1998), (Popa et al, 2002). These works as well as our previous approach (Zhang et al, 2006) suggest that vision-based control is suitable to perform automatic selection of a part and gross motion above the point of insertion, and provide suitable techniques. However, it is difficult to control insertion using vision, because of the very limited depth of focus due to the high magnification of the optical microscope.

A review (Chapter 2) of micromanipulation systems literature shows that at least a combination of force and vision information is needed for implementing automated operation. This thesis carries out the first steps towards the automation. The objectives are:

- To carry out systematic literature reviews on microassembly systems as well as micro force sensing techniques.
- To design and fabricate a new gripper.
- To analyze the force the gripper encounters during the assembly process.
- To design and fabricate the force sensor and integrate it to the system.
- To implement a force control of the assembly process.
- To implement and evaluate the new system for scaffold microassembly.

The automation of the microassembly system needs the integration of vision and force information, and this thesis realizes the first steps of this objective. The assembly system was modified both in hardware and software, which includes replacing two side-view

microscopes with one top-view microscope, replacing the gripper previously used with a smaller one which will avoid the occlusion of the view, design and fabrication of the force sensor, revising the control interface, integrating the whole system and evaluating it by doing some assembly experiments.

1.4 THESIS ORGANIZATION

This thesis is organized as follows. Chapter 2 first reviews the current microassembly systems, and two main categories: master-slave systems and automatic assembly systems are presented. Then some main micro force sensing techniques as well as their applications are reviewed, including piezoelectric sensors, piezoresistive sensors, capacitive sensors and some optical sensors. Chapter 3 describes the design and prototype fabrication of the force sensor integrated into the micro probe gripper. Chapter 4 presents the dedicated desktop workstation used in the assembly task. A force-based admittance controller is implemented in the grasping and assembling process. Then the system is evaluated through scaffold assembly experiments, and a multi-layer scaffold is successfully assembled. Finally chapter 5 concludes the work and proposes some research directions for improving the proposed assembly technique.

Chapter 2

Literature review

2.1 INTRODUCTION

The trend toward miniaturization and high complexity makes it impossible to fabricate the hybrid micro-scale devices in traditional ways. Recently, microassembly has been proposed as a means to fulfill this need, while maintaining high yield and low cost (Brussel et al, 2000). Scaling effects make the microassembly quite different from the assembly in macro world, especially the forces in the micro world, which makes the micro force sensing techniques the key to the automation of microassembly systems. The review of the literature concentrates on microassembly systems and micro force sensing techniques.

2.2 LITERATURE REVIEW OF MICORASSEMBLY SYSTEMS

The scale difference between the micro- and macro-world and the required precision associated with assembling micro parts under a microscope ask for advanced microassembly tools. According to the sequence of the micro parts to be assembled, the assembly systems can be categorized as serial microassembly, parallel microassembly and stochastic microassembly (Cohn et al, 1998). Since the assembly strategy we are using is

serial, the review of the literature concentrates on the serial microassembly relevant studies. The assembly systems can be generally categorized into two methodologies, including master-slave systems and automatic assembly systems (Brussel et al, 2000).

2.2.1 MASTER-SLAVE SYSTEMS

When the size of the articles to be treated is too small, human being can no longer see or feel it. Thus the work cannot be done in the same manner as in the macro world. In such cases, teleoperation with scaling function is a solution to such problems, and master-slave system is one example of such systems. Master-slave systems make the target's scale to be equal to our scale virtually. Thus, the human operator can control the slave manipulation systems by maneuvering the master manipulator (Kaneko et al, 1995). Because of the superior capabilities human has, such as objects discrimination, adaptation to changing tasks, etc., this kind of assembly technique is widely used in life and biomedical field, especially in small batch production.

The research on scaled master-slave systems can be traced back to the early 1990s, and among them a bilateral controlled master-slave manipulator system has been developed by Kobayashi (Kobayashi et al, 1993). Force, position and time scaling control methods were proposed, and a bilateral control of the former two was realized by a micro-macro telemanipulator. Strain gauges were used in both the master-grip and the slave-tweezers, to measure the force that was added to the grip body and to measure the reaction force of the target, respectively.

Scaled master-slave systems started to be extensively studied since it was proposed to be used in biomedical purpose (Ikuta K. et al, 1994). A micro master-slave system was proposed using force and position bilateral control, as well as “dither” technique, which is proposed to improve the controllability of the system against friction. A remote minimally invasive surgery (MIS) was implemented using the above system to verify its biomedical use.

A micro-macro system using the control scheme based on force feedback bilateral control with scaling transfer function gains was proposed and verified by some experiments in (Kaneko et al, 1997). The control scheme provides the operator with the impedance shaped out of the real one, the ratio of which was determined by the products of the force scaling transfer function gain and the position scaling transfer function gain. This makes the control scheme quite simple and suited for real systems and real-time control, and also makes it more effective than the conventional bilateral control schemes.

Carrozza (Carrozza et al, 2000) developed a master-slave system aimed to study the force control strategy in the micro gripper. A strain gauge integrated LIGA micro gripper was used in experiments, and a model in the idling condition was derived, a study of which indicates that an integrative action in control is needed to reach stability.

Literatures after 2000 show that master-slave systems are mainly used in biomedical purpose, and most of the researches are proposed for such purpose. A master-slave type tele-surgical system with intelligent user interface was development by Mitsuishi

(Mitsuishi et al, 2000). Multi-circular guides and “anti-shadow” techniques were adopted in the control of the system to achieve the accuracy, rigidity of the slave manipulator and the controllability of the system, and with these the suture of a 0.3 mm diameter micro-blood-vessel was achieved. Wang (Wang et al, 2005) developed a master-slave robot system with force feedback for micro-surgery, and the validity of it was proved by implementing the system on vas suture experiment on some animals. A 3-DOF scaled micro-macro manipulation system was implemented by Speich and Goldfarb (Speich and Goldfarb, 2005). The transparency bandwidth and the stability of the manipulator pair was improved was achieved by using the loop-shaping compensators, which is enabled by linearizing the feedback, and the results was demonstrated by experiments. A new method for visual feedback for scaled teleoperation was proposed by Clanton (Clanton et al, 2006). In this research the human operator manipulates the handle of a remote tool in the presence of a registered virtual image of the target in real time. This method uses the concept of a new medical device called Sonic Flashlight, which removes the in situ image devices and makes the others objects in the workspace visible.

2.2.2 AUTOMATED ASSEMBLY SYSTEMS

Along with the rapid development of the fabrication techniques, more and more complicated micro devices are widely used, which needs the microassembly systems to be more precise, more efficient, and less costly. To fulfill this need, automatic assembly systems are adopted extensively in those large batch productions. The in-depth study on automatic microassembly systems can be traced back to more than 10 years ago, and at that time there are some precise microrobots commercially available, such as MINIMAN

(MINIaturized MANipulator), PROHAM (Piezoelectric RObot for HAndling of Microobjects), SPIDER I & II, etc. Those microrobots were almost all piezoelectric actuated to achieve high resolution to several nanometers and capable of traveling over long distance. And since then, more and more dedicated automatic microassembly systems were designed and implemented to accomplish more complicated and difficult tasks. Firstly only vision feedback was used (Sulzman et al, 1997), (Fatikow et al, 1999), etc., and later force information was added to achieve faster and more accurate assembly (Fung et al, 2001), etc.

An automatic micromanipulation desktop station equipped with piezoelectrically driven microrobots was developed by (Fatikow and Rembold, 1996). The microrobot was placed on the x-y-table of a highly precise microscope. A fine movement with the resolution of 10 nm can be achieved with the speed of several millimeters per second. A CCD camera was used in the visual servo system to guide the endeffector positioning and micromanipulation.

A microassembly station based on several mobile piezoelectric actuated microrobots was presented by Seyfried (Seyfried, 1999). The microrobots performed the motions and micromanipulation under the force control through several vision sensors either on an X-Y stage under a microscope or in the chamber of a scanning electron microscope (SEM). With the multi-robots system, the microassembly task can be achieved in parallel.

Wafer-level 3D microassembly workcell equipped with piezoelectric force sensor was developed and experimented by Ge Yang (Ge Yang et al, 2001), (Ge Yang et al, 2003). This station consists of several independent components: a multiple-view imaging system, a piezoelectric force sensor, a 4 DOF micromanipulator, a 4 DOF positioning system, and a flexible micro gripper. To achieve high reliability and efficiency, the wafer was set on a vertical mount, and force feedback was applied as a complement to vision control to achieve high precision, which has seldom been studied before.

The idea of "Ortho-tweezers" was first used in the design of the gripper by Thompson (Thompson and Fearing, 2001), to realize a full automatic robotic microassembly. "Ortho-tweezers" gripper means the two finger of the gripper were orthogonal, which is more easily implemented in the micron scale systems than anthropomorphic design. Strain gauges were used in the force sensing module to facilitate the visual control to achieve more accurate, faster motion. Sticking effects were also considered in the releasing process.

Quan Zhou (Quan Zhou et al, 2002) developed a microassembly station in the purpose of studying the influence of the ambient environmental parameters on microassembly. During the experiments, the environmental temperature and humidity, the mechanical vibration and air flow were changed, thereby causing the adhesion forces, the microassembly system and the assembly system to change. The results showed that environmental parameters affected the precision of the microassembly process as well as the instruments used significantly.

Adhesion effect based dynamic micromanipulator was used in the microassembly system developed by Haliyo (Haliyo and Regnier, 2003) (Haliyo et al, 2002). High surface energy material was used in the endeffector to achieve the successful gripping, and the releasing was achieved by control the inertial effects both of the endeffector and the objects, which was used to overbalance the adhesion forces.

A non-contact type microassembly system using centrifugal force suitable for micro-opto-electro-mechanical applications was proposed and demonstrated by Lai (Lai et al, 2004). Centrifugal force was adopted because it will evenly distribute on the micro parts to be handled, thus will not destroy the parts easily. The assembly process is quite simple which makes this method low-cost and reliable. During the rotation, most of the hinged micro parts will be released and automatically lock themselves to the designed latches, thus to achieve the self-assembly. And experiment results showed that this task specialized method can give 100% yield without destroying any single micro part.

Remote center compliance (RCC) unit was used by Yong-bong Bang (Young-bong Bang et al, 2005) in a microassembly system. A shape memory alloy actuated gripper was adopted to achieve the grasping. A low translational and rotational stiffness micro RCC unit was deployed in a peg-in-hole type assembly task to achieve the compensation of the alignment error between the peg and the hole. And the force sensing was achieved through the implementation of a voice coil motor (VCM) drive mechanism.

Transparent electrostatic gripper was used in a novel microassembly system developed by Enikov (Enikov et al, 2005). Several different sensing modalities including computer vision, a fiber-coupled laser, and a position-sensitive detector, were used to achieve precise position control. Reflected intensity distribution modeling was used in the computer vision processing part to distinguish the transparent gripper from the objective, especially when they lap together. Two control algorithms were shown in the alignment of the micro parts, and the hill-climbing algorithm was proved to be more accurate than the spatial gradient method in a peg-in-hole type task.

Due to their different principles, master-slave systems and automation systems have their own characteristics, and by taking their advantages, they are used for different purposes. The details are shown in Table 2.1.

Table 2-1 Comparison between master-slave systems and automatic systems.

	Master-slave systems	Automatic systems
Automatic level	Human operator involved during the whole process	Human operator free
Sensing modalities	Vision, Haptic, Sound, all those can be fed back to human	Vision, force, position, all those can be feedbacked to machine
Cost	High	Low
Efficiency	Low	High
Task batch	Small	Large
Flexibility	High	Low
Applicable field	Life science, Biomedical mainly	Widely, almost all kinds of microassembly tasks

According to these prior studies, the advantages of the automatic assembly system proposed and implemented in this thesis can be summarized as follows:

1. Realize a fast and precise movement of the gripper;
2. Allow position error during the assembly process;
3. Realize real-time force control of the movement of the gripper;

And the purpose of this thesis is to automate the previously used human-operating system. With this new system, a faster, more precise and high yield assembly can be realized, and furthermore, various architectures of scaffold can be obtained.

2.3 LITERATURE REVIEW OF MICRO FORCE SENSING TECHNIQUES

Because of the scale difference, microassembly tasks are always achieved under some optical or electron microscopes. However, with only the vision information the repeatability of the system cannot be better than submicron, and the lack of interaction information may lead to the breaking or damaging of the micro objects in work space. Thus a second non-visual sensing modality, such as force sensing, must be used to achieve better performance of the microassembly process. And depending on the sensing principles used in them, the most popularly used force sensing technologies can be categorized as piezoresistive sensing, piezoelectric sensing, capacitive sensing, and optical techniques based sensing etc. (Fahlbusch and Fatikow, 1998), (Nelson et al, 1998).

2.3.1 PIEZORESISTIVE SENSING (STRAIN GAUGES)

Piezoresistive sensing utilizes piezoresistive effect which describes the changing electrical resistance of a material due to the applied stress. When a sensor of this type is connected in a circuit, the current through it or the voltage over it will change when it was deformed. Hence, the force can be found through measuring this change.

The change of resistance of metal devices due to an applied mechanical load was first discovered in 1856 by Lord Kelvin. With single crystal silicon becoming the material of choice for the design of analog and digital circuits, the large piezoresistive effect in silicon and germanium was first discovered in 1954 (Smith 1954).

Strain gauges can be constructed based on resistance, capacitance and inductance. But the application of strain gauges based on the latter two principles is limited by their sensitivity to vibration, mounting requirements, and circuit complexity. Hence, strain gauges based on resistance are mostly widely used.

A pair of metal-foil strain gauges was used for force control in a teleoperated microsurgery system (Ku and Salcudean, 1996). Two gauges were attached to the two fingers of the micromachined gripper, and the signal from the gauges was amplified by an instrumentation amplifier circuit. Temperature compensation was achieved by using the two gauges to form a half bridge and using pulsed excitation to the bridge. The sensor was calibrated by hanging known weights off the tip of each of the gripper arm. Then through

the haptic device in the master-slave system, the surgeon can feel the scaled gripping force from the operating site just as if he was operating the objects directly.

Integrated strain gauge was used in a microtesting system developed by Ruther (Ruther et al, 1997). The whole testing system was quite small and it was manufactured by standard LIGA-process. The strain gauge was directly fabricated on the silicon substrate, and then covered by the other microstructure of the actuator. A piston with diameter of 2 micrometers was attached in the middle of the gauge grid, which was used to touch the object and transmit the force directly to the strain gauge. The bending displacement of the tested object caused by the touching of the piston was detected by an optical position sensor, and the accuracy of the testing system can reach 200nm.

A multi-axial force sensor made from strain gauges was used by Arai (Arai et al, 1998) in a contact type micromanipulation system in liquid. The sensor chip used in the system was made by silicon micromachining, and there are two strain gauges fabricated on each of the four cantilevers of the chip, which was designed to suspend the center mass of it. Each pair of the gauges made up a half bridge, and the output voltages from the four bridges, together with the applied moments and compliance identified by experiments were used to calculate the force.

PI force control of a micro gripper was realized by Eisinberg (Eisinberg et al, 2001) by using semiconductor strain gauges in a biomedical microdevices assembly system. Detailed integration and characterization process of semiconductor strain gauges used in the system were presented. The integration process includes accurately cleaning the

attaching surface, applying the adhesion layer, abrading the cured precoat surface, bonding the strain gauge, and electrical connections. Each step must be given attention, for the quality of the finished assembly is dependent on the correct process, and modifications must be made according to special requirements. PI force control was achieved based on the model from the characterization, which provided the strain gauges' responses in the idling and grasping period.

An assembled miniature three dimensional force sensor based on semiconductor strain gauges was developed by Berkelman (Berkelman et al, 2003) for microsurgical purpose. The sensor consists of an outer hollow cylinder joined to an inner cylinder by eight thin flexible beams, and all the parts were fabricated using electrical discharge machining (EDM) to achieve superior mechanical properties. Strain gauges were attached to the beams, and double-cross flexible beam configuration was applied to achieve uniform sensitivity to forces in all directions. Calibration using standard loads showed good linearity in all axes, and an experiment in a scaled master-slave system was successfully achieved.

Adaptive zero-phase error tracking controller (ZPETC) was designed and implemented by Jungyul (Jungyul Park et al, 2004) using two strain gauge sensors in a micromanipulation system. A two finger micro gripper was used in the system for manipulation micro soft objects such as biomaterials and tissues, which require real-time control of the gripping force to avoid the invasion of the target material by excessive force. An empirical model was obtained based on the system identification technique, and besides the feedback loop,

adaptive ZPETC was adopted to realize the trajectory control. Experiments results showed that using the adaptive ZPETC method, gripping force can be controlled despite the change of the target and variation of the actuating force due to aging of the system.

Piezoresistive effect based sensors have resolutions in micro Newton or sub micro Newton ranges and are suitable for real-time measurement, but this also leads to one disadvantage: time dependency of the measurement, which means it is not suitable for static load measurement, and because of its principle of sensing, its performance is also limited.

2.3.2 PIEZOELECTRIC SENSING (“SELF-SENSING”)

Piezoelectric sensing is based on the piezoelectric effect of piezoelectric materials. The electrical charge change is generated when a force is applied across the surface of a piezoelectric film.

In 1880, the brothers Pierre Curie and Jacques Curie predicted and demonstrated piezoelectricity using tinfoil, glue, wire, magnets, and a jeweler's saw. They showed that crystals of tourmaline, quartz, topaz, cane sugar, and Rochelle salt (sodium potassium tartrate tetrahydrate) generate electrical polarization from mechanical stress. And among all the piezoelectric materials, polyvinylidene fluoride (PVDF) is most widely used because of its low-Q response, ease of use, compliance and high sensitivity, and almost all the piezoelectric sensor used in the researches were made in this material.

A micromachined tactile sensor made of PVDF film for minimally invasive surgery (MIS) was presented by Dargahi (Dargahi et al, 2000). Integrated with the endoscopic grasper, the sensor consisted of three layers: plexiglass substrate, PVDF film, and silicon tooth. The fabrication and assembly process was done in a cleanroom. Only four channels were used in the sensor array to reduce the crosstalk problems, and using the sensor, both the magnitude and the position of the applied force can be precisely obtained.

Micro touch sensor made of piezoelectric film for microbe isolation and separation was designed and fabricated by Arai (Arai et al, 2004). Fabrication of the sensor was achieved by depositing a piezoelectric thin film on the surface of a titanium pipette and then depositing the sensing electrode and actuating electrode on the piezoelectric film. The sensing was achieved by detecting the mechanical impedance change after the pipette touched the object. Experiments were done to validate the efficiency of the sensor, and with the extreme sensitivity microbe can be extracted without damaging the pipette.

Cell injection force was detected by using piezoelectric force sensor in a microrobotic system (Deok-Ho et al, 2004). The PVDF film was held by a clamping fixture, and the micro injection pipette was bonded to the other tip of the film. Nickel electrodes were deposited on both sides of the film to get the signal. With this setup, a range of hundreds of micro-Newton can be achieved, and experiments results showed that the system can measure cellular force in real-time.

High sensitivity 1-D and 2-D PVDF force sensors were developed for microassembly by Yantao (Yantao et al, 2003, 2004). The 2-D force sensor was fabricated by arranging and fixing two PVDF sensitive pairs perpendicularly, and micro force as well force rate could be detected with resolution in the micro Newton range. Distributed parameter model was adopted in developing of the sensing model, and in-bandwidth method was adopted in the designing of the sensor structure. Furthermore, a zero frequency term was added to the model to compensate for the removal of the higher-order modes (Yantao et al, 2005). Besides the above designed sensor structure, an active structure which was suitable for mounting at the end-effector was developed by using the 1-D PVDF film (Yantao et al, 2005). The sensor consists of an actuating layer of PVDF film additional to the sensing layer, and when the sensing layer sensed the external force, a feedback would be transmitted to the actuating layer through a servo transfer function, and then the actuating layer will generate a counteracting bending moment to balance the deformation caused by external force in real-time. Thus, when mounted at the tip of the end-effector, the active structure can greatly enlarge the dynamic range and the manipulability.

Piezoelectric sensors can reach very high resolution and accuracy, and can achieve real-time force measurement, but the literatures show that the structure of the sensor will affect the performance greatly. This requires that care must be taken in the design and fabrication process for the sensors based on this principle.

2.3.3 CAPACITIVE SENSING

Capacitive sensing makes use of the change in capacitance between two metal plates to convert the information of external force and pressure applied into electrical signals such as changes in current, voltage, etc.

From the literatures, it can be found that deep reactive ion etching (DRIE) process is widely adopted in the fabrication of capacitive sensors, for this technique allow etching deep cavities in substrates with relatively high aspect ratio. The researches in the literatures are all based on this technique, and some other novel microfabrication principle was added to it, as well as different types and structures of capacitors are adopted to fulfill various needs. A multi-degree-of-freedom capacitive force sensor for the purpose of single cell mechanical manipulation was developed by Enikov using DRIE process (Enikov and Nelson, 2000). Wet anisotropic etching along with DRIE was adopted to fabricate the three-dimensional structure of the sensor, and electronics was integrated using flip chip bonding. A pipette can be fixed inside the structure of the sensor, which will allow the moving of the pipette in six-degree-of-freedom. Non-symmetric comb capacitors were used to achieve decoupling between displacements in the x- and y-direction. The z-direction force was sensed through planar electrode under the chip. The following studies were mostly based on the developed macro structure. A transverse mode comb drive was used which greatly improved the sensitivity when the sensor was used for cellular force measurement (Sun et al, 2002). The complete sensor was capable of sensing forces up to 490 micro Newtons with a resolution of 0.01 micro Newtons in x, and up to 900 micro Newtons with a resolution of 0.24 micro Newtons in y. Electrostatic microactuators were

also integrated in the structure so that the system stiffness could be modulated during the sensing process, thereby to increasing the force measurement dynamic ranges (Sun et al, 2003). Differential tri-plate comb drives were used in developing the force sensor for measuring drosophila flight force (Sun et al, 2004). This structure enabled the sensor with high sensitivity, good linearity, compact size, and large bandwidth, which was essential for capturing the aerodynamic and inertial forces of drosophila in real-time.

Capacitive sensors have no hysteresis, better long-term stability and high sensitivity, but a study of the literatures also shows that the fabrication process of the capacitive sensor is really strict, must be completed in the cleanroom, and the structure of the sensor is also customized based on the task.

2.3.4 OPTICAL TECHNIQUES BASED SENSING

Optical techniques such as interference, optical deflection, laser speckle, and holographic interferometry can be used in force sensing with the advantages of electromagnetic immunity, non-contact and high resolution. Nowadays, quite a lot of optical micro force sensing methods are available with high sensitivity and resolution, such as atomic force microscope (AFM), scanning force microscope (SFM), laser Raman spectrophotometer (LRS), etc.

Laser Raman Spectrophotometer (LRS) was first used for force measurement in micromanipulation by Arai (Arai et al, 1996). LRS method was adopted to realize force sensing without using displacement information caused by elastic deformation, which

could improve the stiffness of the end-effector and enhance the manipulability of the system. A two-fingered tweezers equipped with a micro electron discharge machine fabricated silicon cantilever was put inside the Raman microscopic chamber, and the force sensing was achieved by measuring the stress of the cantilever by LRS. Experimental results showed micro Newton level accuracy, and at the same time increase the system stiffness.

Scanning force microscope (SFM) based force sensing system allowing a work temperature of 1.4 K was developed by Weitz (Weitz et al, 2000). The piezoelectric scanning head was a 3-inch piezoelectric tube, which was held in a glass ceramic frame and then encapsulated in a vacuum chamber. The purpose of the proposed SFM was to detect the surface potential, and this was achieved by probing the electrostatic force between the metallized tip of the object and the electrical conducting sample placed inside the SFM head. The setup was well suitable for investigating Hall-potential profiles of a buried two-dimensional electron system (2DES), and can reach the resolution of submicron level.

Specially designed atomic force microscope (AFM) for working in liquid was developed by Zhang (Zhang et al, 2005). Usually optical force sensors are not suitable for working in liquid because of the interference of the surface, but in this system a circular Plexiglas window was used to prevent the effect. When measuring, the objects were immersed in liquid, and the Plexiglas window was put on the liquid surface with an end-effector fixed to its lower surface, and a circular meniscus was established around the window, thus to

achieve the sensing in liquid. Experiments were conducted to demonstrate the validity and efficiency of the system.

Optical methods have very high sensitivity, and can achieve resolutions of sub nanonewton level. But the literatures show not many force sensing system were using optical techniques, this might because there are still difficulties to fully take the advantages of those methods. The optical force sensing systems are very complicated, high cost, and usually have strict environments requirements. Some facilities such as LRS are not suitable for real-time sensing.

Evidence from investigation of the literatures shows that no single micro force sensing technique stands out as being the most promising method and details of a comparison is shown in Table 2-2.

Extensive researches have been done on micro force sensing techniques, but they are seldom realized in the microassembly field; and for those used in such tasks, the sensors are always attached to the tips of the two finger grippers to detect the grasp force. The sensor designed and implemented in this thesis realizes a real-time movement control of the micro probe gripper, and after covered with isolation, it can be used in final applications to assemble scaffolds in liquids.

Table 2-2 Popular force sensing technologies.

	Real-time	Reference	Feature	Application
Piezoresisti-ve (Strain gauges)	Yes	Ku 1996	metal-foil strain gauges / half bridge / range: dozens of mN / Resolution: sub mN.	Microsurgery
		Ruther 1997	single strain gauge / range: 30 mN	Young's modulus testing
		Arai 1998	8 strain gauges made up four half bridges / three-axial sensor chip	Contact type micromanipulati on in liquid
		Eisinberg 2001	semiconductor strain gauges / range: 22mN / resolution: mN / PI force control	Assembling biomedical microdevices
		Berkelm-an 2003	assembled semiconductor strain gauges / range: 500 mN / resolution: sub mN	Robot-assisted manipulation
		Jungyul 2004	two semiconductor strain gauges / adaptive ZPETC / range: dozens of mN	Manipulation of soft materials
Piezoelectric	Yes	Dargahi 2000	high sensitivity / large dynamic range / wide bandwidth / good linearity / high signal-to-noise ratio / range: 2N	MIS
		Arai 2004	high sensitivity / impedance detect / high rigidity / excellent durability	Microbe isolation and separation
		Deok-Ho 2004	high linearity / high signal-to-noise ratio / range: hundreds of micro Newton	Cellular force measureme-nt
		Yantao 2003, 2004,2005	in-bandwidth model with zero frequency term compensation / actuating layer for counteracting bending	Mounted at the end-effector
Capacitive	Yes	Enikov 2000, Sun 2002, 2003, 2004	multi-DOF / non-symmetric comb capacitors / wet anisotropic etching / transverse mode comb drive / actively servoed / tri-plate	Single cell manipulate-on / drosophila flight force measureme-nt
Optical	Not all suitable	Arai 1996	LRS / measuring small area (1 micrometer) / highly precise	Micromani-pulation
		Weitz 2000	SFM / low-temperature / resolution: submicron	2DES study
		Zhang 2005	AFM / work in liquid	Manipulati-on in liquid

Chapter 3

Force sensor integrated micro gripper

3.1 INTRODUCTION

As has been described in chapter one, the mission of our microassembly task is to transfer home-made micro parts from its original substrate wafer to the target wafer containing the structure of zero-plate, which contains parts fabricated on the wafer to hold the first layer of scaffold. The assembly process used to be accomplished by a human operator using the desktop microassembly system (Figure 1-1A) under the guidance of only the side view of the work space (Figure 3-1) from two microscopes.

A B

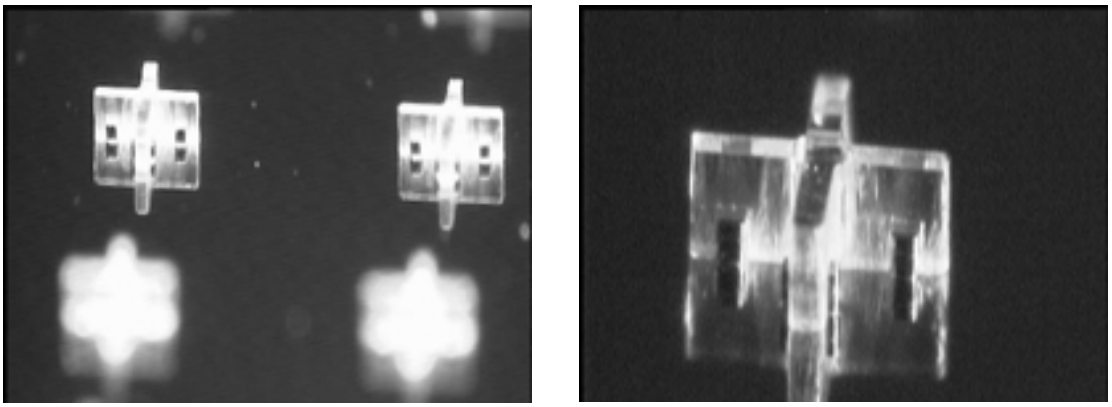

Figure 3-1 (A) Side view of multiple parts. (B) Side view of single part.

To automate the system, the strategy is to add a force sensing module besides the visual feedback. Vision will be used to locate the micro parts on the wafer and to find the spot to put the part, i.e., to guide the movement in the direction parallel to the wafer, and the force will be used to control the grasping process of the parts, i.e., the movement in the direction vertical to the wafer to reach the parts and the grasping and releasing of the parts.

To locate the micro parts on the wafer, the edge of the part is the only distinguishable reference in the image. But it is impossible to precisely identify a single part on the wafer using the previous setup. This is because the side view of the work space cannot give a clear image of a single layer of the micro parts to be assembled or already assembled, and this makes it difficult to find the edge of a single part. And the condition becomes worse after some parts have been assembled on the wafer (Figure 3-2).

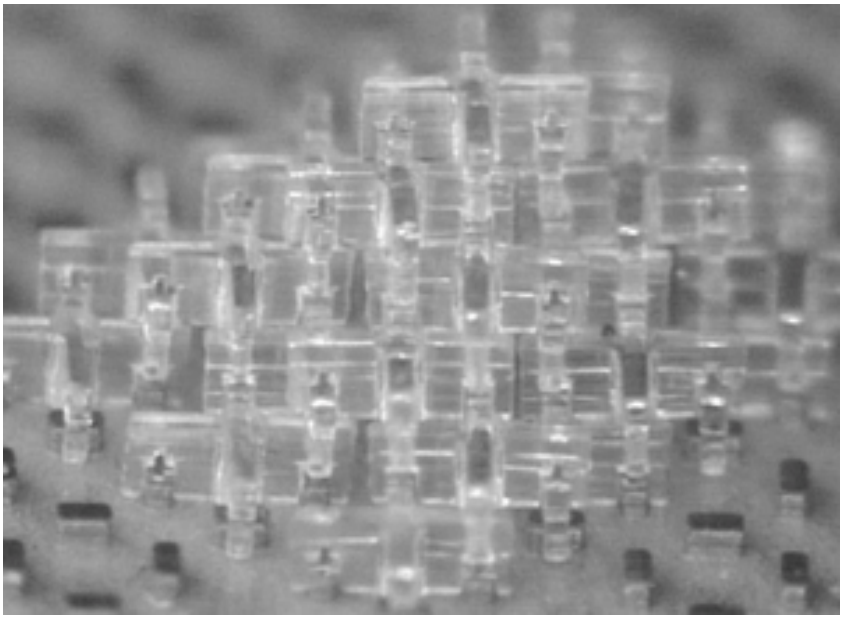

Figure 3-2 Side view of the wafer containing the zero-plate and a scaffold.

A top view of the work space (Figure 3-3) can solve this problem, and to achieve the top view a microscope must be fixed right above the stage holding the wafers instead of the previous configuration.

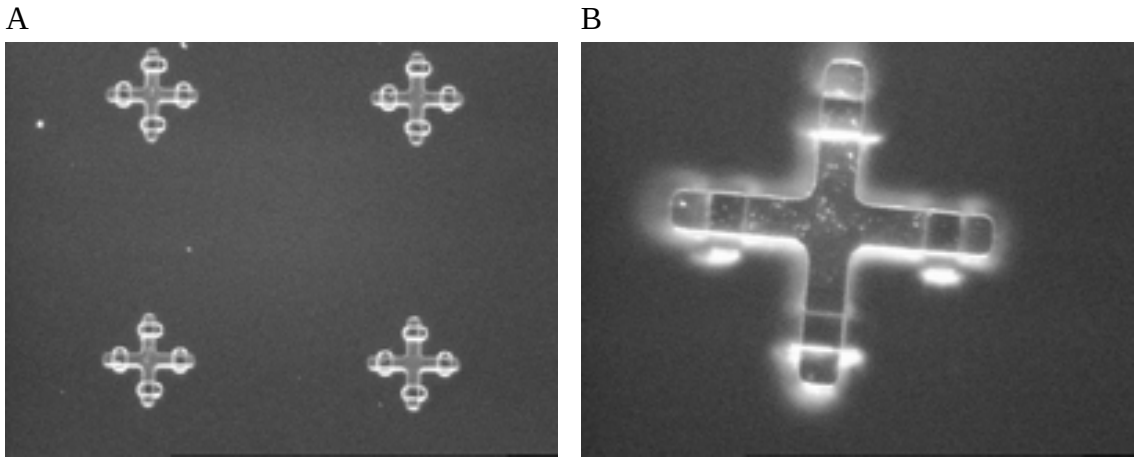

Figure 3-3 (A) Top view of multiple parts. (B) Top view of single part.

To fulfill this purpose, the old shape memory alloy (SMA) gripper must be replaced for the following two reasons:

- The gripper is too big compared to the micro parts (Figure 1-1C), and the structure that interfaces it to the moving stage is even bigger, which make it difficult to fix a microscope above the wafer, and it also occlude the structure below it.
- In our strategy, the touching down phase of the gripper is controlled by a force sensor, and the structure of the old gripper doesn't allow the integration of a force sensor for measuring the force in assembly direction.

Another reason for replacing the old gripper is that it cannot grasp the micro parts in a balance state. The cross-shape part has four branches, but the design of the SMA gripper allows the grasping of only one of them. This leads to an unbalance of the part when the part is lifted as well as when it is pushed down on the wafer, and this results in the tilt of the part.

3.2 ASSEMBLY FORCE ANALYSIS

From the previous description of the assembly task, the gripper will be involved in the following two phases: (1). Picking up the parts from the substrate wafer; (2). Assembly the parts to the zero-plate wafer. Hence, the forces the parts encounter during the whole process are as follows:

- *Gravitational force* (f_g): The gravitational force of the micro parts always exists, and it is one of the forces that the grasping force from the gripper should counteract during the grasping phase, and also one of the forces that counteract the grasping force in the releasing phase.
- *Adhesive forces* (f_{a1}, f_{a2}, f_{a3}): When the parts to be handled are less than one millimeter in size, adhesive forces between the gripper and the object can be significant compared to gravitational forces (Fearing, 1995). These adhesive forces arise primarily from surface tension forces, van der Waals forces, and electrostatic forces. A comparison of the gravitational force to the adhesive forces acting between spherical object and plane is shown in Figure 3-4. It is assumed that the object is a silicon sphere picked up by a gripper with flat jaw surfaces.

In our case, the micro parts we are using have the dimension of $500\times500\times200$ microns, and so the adhesive forces exist between the parts and any surfaces they contact during the assembly process. These include the substrate, the gripper, and the zero-plate. And the order of the forces can be approximately derived from the curve in Figure 3-4.

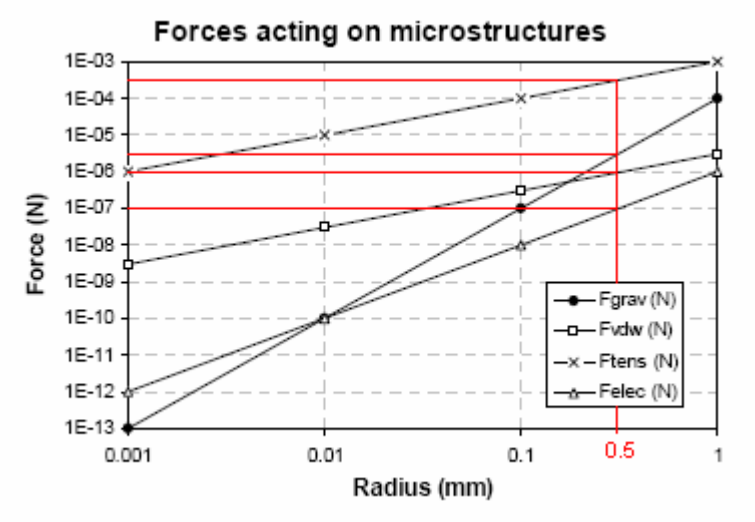

Figure 3-4 Gravitational, van der Waals, surface tension, and electrostatic forces between sphere and plane (Fearing, 1995).

The van der Waals force is of the same order of the gravitational force but a little smaller, while the electrostatic force is one order lower than the gravitational force. The surface tension is much larger than the gravitational force. Thus the surface tension may disturb the assembly process greatly, and the force as shown in the figure was calculated by the formula as follows (Fearing, 1995):

$$F_{tens} = \frac{\gamma(\cos\theta_1 + \cos\theta_2)A}{d} \tag{3.1}$$

where γ is the surface tension ($73mNm^{-1}$ for water), A is the shared area, d is the gap between surfaces, and θ_1, θ_2 are the contact angles of the liquid with the two surfaces. From the formula, it can be seen that the surface tension will decrease with low humidity, and small radii of curvature. Other factors like contact time and hydrophilic surfaces can also greatly affect the surface tension. Due to different environmental and coating factors, the surface tension in our case may be quite different from the one shown in the figure above, and it is almost impossible to calculate the force accurately. Experiments were implemented by using the old SMA gripper to measure the effects of the adhesive forces, and during the grasping and releasing phase of the assembly, no disturbance from the adhesive forces was found.

- *Connecting force* (f_c): This force exists between the micro parts and the original substrate wafer. During the fabrication process of the micro parts, there is a small part of the oxidation layer under the parts not etched off for the purpose of holding the part on the wafer, consequently keeping all the parts on the wafer align in the same direction. This dimension of the connecting part can be controlled by adjusting the oxide etching time, thus approximately controlling the connecting force.
- *Grasping force* (f_{gp}): The force produced by the gripper should be enough to counteract the forces tending to hold the parts on the original substrate wafer and pick the part up during the grasping phase. If it still acts on the part during the releasing phase, it must be moderate so as not to prevent the part from releasing from the gripper.

- *Pushing force* (f_p): This force is usually generated by the structure of the micro gripper, and it is the main force that pushes the micro part down on the target wafer until it is assembled stably.
- *Friction* (f_{f1}, f_{f2}): During the assembly, the parts in the upper layer are pushed into those in the lower layer or the zero-plate, and the friction is produced between the wall of the lower layer structure and the notches on the upper layer of parts. The friction between layers is the main force that releases the parts from the gripper and then keeps the parts in their positions. And the friction can be controlled approximately by changing the gaps between the structures of the parts, i.e., changing the thickness of the wall or/and the width of the notch.

A detailed description of the above listed forces during the two main phases of the assembly process is shown in Table 3-1.

And to realize a successful assembly, the forces listed above should follow some rules. In the picking phase:

$$f_{fp} + f_{a2} > f_g + f_{a1} + f_c \tag{3.2}$$

And for the assembling phase:

$$f_p + f_g > f_{a3} + f_{f1} \tag{3.3}$$

$$f_{f2} + f_g + f_{a3} > f_{gp} + f_{a2} \tag{3.4}$$

Thus the new design of the micro gripper should ensure that the grasping force (f_{gp}) produced by the gripper meet the requirement as:

$$f_{f2} + f_g + f_{a3} > f_{gp} + f_{a2} > f_g + f_{a1} + f_c \tag{3.5}$$

Table 3-1 Forces during main assembly process.

Phase	Force	Direction	Remarks
Pick	f_g	down	Gravitational force of micro part.
	f_{a1}	down	Adhesive forces between part and substrate.
	f_{a2}	up	Adhesive forces between part and gripper.
	f_{gp}	up	Grasping force generated by the gripper.
	f_c	down	Connecting force between part and the substrate produced by the oxidation layer.
Assemble	f_g	down	Gravitational force of micro part.
	f_{a2}	up	Adhesive forces between part and gripper.
	f_{a3}	down	Adhesive forces between part and substrate.
	f_{gp}	up	Grasping force generated by the gripper.
	f_p	down	Pushing force generated by the gripper.
	f_{f1}	up	Friction during the pushing down period.
	f_{f2}	down	Friction during the releasing of the gripper.

The above inequations were derived based on the assumption that the grasping force (f_{gp}) produced by the gripper acts on the micro parts all the time, i.e. the grasping force acts on the parts during the picking phase as well as the assembling phase.

For the condition that the grasping acts on the parts only during the assembling phase, equation (3.5) should be revised as:

$$f_{gp} + f_{a2} > f_g + f_{a1} + f_c \tag{3.6}$$

Using a micro balance, experiments were carried out to measure those forces related to the design of the new gripper. The force that the gripper needs to produce to pick up the part from the wafer is 0.02N, and the force needed for the part to be assembled to the zero-plate is 0.1N.

3.3 DESIGN AND FABRICAITON OF MICRO GRIPPER

3.3.1 GRIPPING STRATEGY

From the analysis mentioned in previous sections, it can be derived that the open-close type gripper is not suitable for our assembly task, for it is too big compared to the micro parts, and it will lead to an unbalance of the grasping. Thus a new gripping strategy must be adopted for the gripper to fulfill those requirements. Besides the specific requirements of the gripper for our microassembly task, there are some common important requirements as listed in Table 3-2 for micro grippers, which our gripper design should fulfill.

On the basis of the above listed requirements, various gripping strategies can be used in the microworld (Table 3-3).

The above listed gripping strategies has their special applications, However many of them can hardly provide a stable grasp and require a significant time to grasp or release a part. We experienced that even with the dedicated two-finger gripper developed in (Zhang et al, 2001), although it provided a relatively stable grasp, the micro parts orientation was difficult to maintain during insertion. Further, the gripper should be small as to not prevent

vision control of the gross motion. The inspiration of the new design of the micro gripper comes from the peg insertion tasks, which has a long history in the field of robotics and automation research (Nakagaki et al, 1995) , (Hara et al, 1997), (Bruzzone et al, 2002). For the shape of the mating part is very simple and geometrically well defined, the peg-in-a-hole task is one of the most commonly used goal tasks in macro world, and many practical macro assembly tasks include such insertion tasks. Such a strategy can be adopted in our micro assembly task for the following main seasons:

- *Feasibility*: A peg insertion task needs mated peg and hole. The micro part used in our scaffold assembly task contains a plane with the dimension of about 100×100 microns. It can be enlarged to fabricate a hole in it, which is quite simple through photolithography technique. The diameter of the hole can be controlled precisely, thereby ideal friction between the peg and hole can be obtained. Some modified micro parts have been fabricated, and a comparison is shown in Figure 3-5. The detailed fabrication process will be explained in the next chapter.
- *Simplicity*: With only one finger, the micro probe gripper can be made very thin to avoid occluding the top view of the work space. The grasping force is produced by inserting the peg in the hole, so no extra actuator for the gripper is needed. The probe micro gripper can be mounted to the vertical linear stage so that it can be moved vertically.
- *Geometrically stability*: The hole can be fabricated in the geometrical centre which is also the mass centre of the micro part, and thus balanced grasping can be achieved.

Table 3-2 Important requirements for micro gripper design (Fischer et al, 1997).

Requirements
Low weight
Small space
Controlled, exactly doable gripping force
Freely positioning gripping jaws
Possibility for sensor integration
Possibility for visual assembly monitoring
High assembly speed and short cycle times respectively
Good continuous use behavior
Suitability for automated assembly
Separate gripper control also applicable for sensor processing

Table 3-3 Popularly used gripping strategies (Brussel et al, 2000).

Type		Application	Limitations
Contact	Mechanical gripper	Usually big size parts.	Need precise force gripping force control.
	Adhesive gripper	Parts less than 1mm in size.	Sticking effects are difficult to control, may disturb the process.
	Vacuum gripper	Small dimension needed situation, parts have smooth surface.	The tube has to been very thin, so easily obstructed.
Non-contact	Aerostatic gripper	Contact-sensitive, surface-structured parts.	High cost, complicated system.
	Magnetic field		
	Electric field		

- *Possibility for sensor integration*: The probe micro gripper can be made to L-shape, and the vertical part (the probe) can be used to pick the micro part while the horizontal part (the cantilever) can be used to integrate the force sensor, which makes the sensing of the contact force possible.

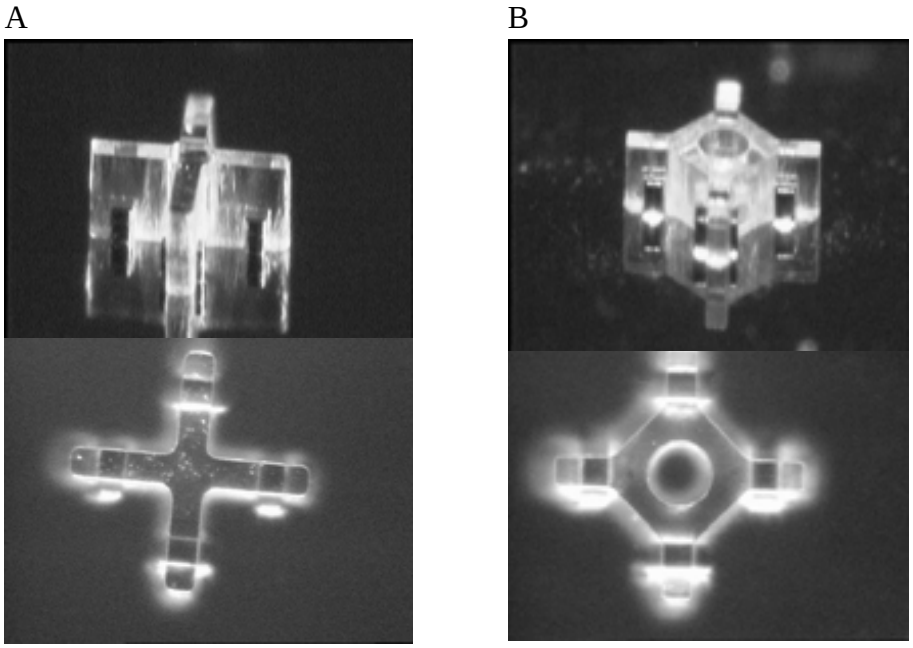

Figure 3-5 (A) Old part. (B) New part with a hole.

3.3.2 GRIPPER DESIGN

The structure of the proposed L-shape micro gripper is shown in Figure 3-6. As the tip is inserted into the hole in the part in order to grasp it, the pushing shoulder provides the pushing force during the assembling period. The sensor is attached to the cantilever.

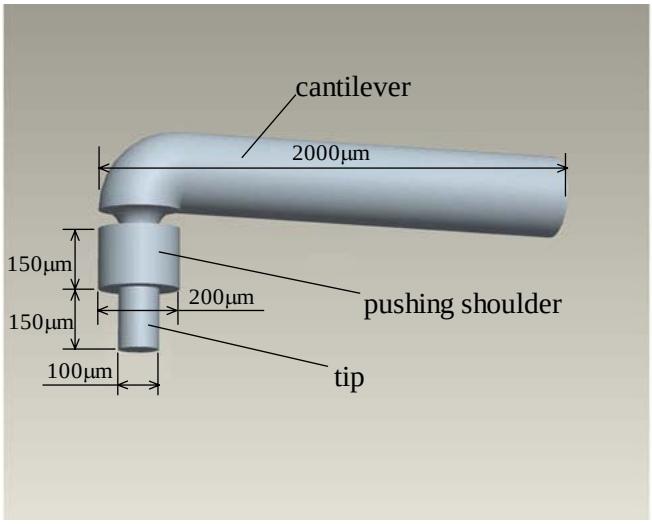

Figure 3-6 L-shape micro probe gripper.

The first version of the gripper is just the cantilever and the tip, without the pushing shoulder, and the pushing force was generated by the tip itself. Fabricated through electrochemical etching technique (the fabrication process will be described in detail in the next section), there will be a slope at the gripper tip. The gripper can work without the pushing shoulder, but there are some problems during both the grasping and the assembling process:

- *During the grasping process:* The gripper lifts the part by insertion, and since the part has to be released during assembly, the friction between the tip and the hole must not be too large. Hence, the gripper cannot be inserted into the hold too tightly, and there can be relative movement between them. Without a pushing shoulder, there is no constraint between the gripper and part that can prevent the gripper tip to be inserted more into the part, thus lead to an increase of the friction between them and cause failure of the release. And as observed during some grasping experiments, the part tilted after it was picked up, which would bring difficulty to the assembly process.

- *During the assembly process:* The assembly is achieved by pushing down the parts on to the wafer from above, and without the pushing shoulder, the assembly action would be accomplished entirely by the friction between the gripper tip and the hole. As described above, after the grasping, the part was not tightly connected to the gripper. During the assembly process, while pushing the part on to the lower structure, the gripper tip would be inserted into the part more, resulting in an increasing in the friction between the gripper and the part. Hence, it will be difficult or impossible to release the part from the gripper.

A sharp pushing shoulder can solve the above listed problems, and the design of the dimensions of the gripper obeys the following several considerations beside those general requirements:

a) The tip (Figure 3-6) should have the dimension that matches with the hole in the part, i.e., it should have a moderate diameter, with which it is able to provide enough friction between the tip and the hole for picking the parts up, and at the same time, the tip cannot be too thick, which will cause the friction to exceed the ideal value and disturb the releasing action.
b) The assembly strategy uses the top view of the workspace to guide the locating of the movement in x-y plane, so the gripper cantilever (Figure 3-6) must be thin enough and long enough not to disturb the vision.
c) The angle between the gripper tip and the cantilever is designed to be 90 degrees, as shown in Figure 3-6. During the insertion process and the assembly process, when there is force applied to the gripper tip, the cantilever will bend, and the tip will turn

at the corner correspondingly to keep its original angle relative to the cantilever. While the tip is inserted in a part, the trend of the movement will cause deformation of the micro part. The parts used in the assembly experiments are made from SU8, which is very fragile after the photolithography process (the detailed fabrication process will be presented in next chapter), and excessive deformation will cause plastic deformation to the part or even break it. So, ideally the deformation in the cantilever's free end should be controlled in a safety range. This requires the gripper must be made from some stiff material, and the length of the cantilever should not exceed the safety range.

Following steps were taken to design the ideal micro probe gripper:

1. *Material selection*:

   An investigation of the literature shows that tungsten is most widely used in micro probing devices. Tungsten probe cards are conventionally used in wafer-level testing to check defects in Integrated Circuit, and the tip can provide a stable contact with diameter down to 15 microns (Maekawa et al, 2000), (Chao et al, 2003). The same size tungsten probe was also used in microassembly and nanoassembly process (Skidmore et al, 2004). It is used for nanostructure assembly, and the tungsten probe tip can be etched to 10 nm radius, but still can provide enough force for grasping. Tungsten is also one of the most popularly used materials in scanning probe microscopy (SPM) such as scanning tunneling microscopy (STM), atomic force microscopy (AFM), for its superior mechanical properties and electro chemical properties.

As the requirements for the probes used the above mentioned researches and applications match those for our task, tungsten was selected for its high stiffness, good mechanical properties and easiness for machining. Experiments and analysis were carried to demonstrate the feasibility of using tungsten.

2. *Gripper probe design*:

The gripper probe (Figure 3-6) is composed of the gripper tip and the pushing shoulder. The tip is used to insert into the hole in the part and pick up the part with friction, so the medial diameter of the tip is designed to be $100\mu m$. The tip is designed to be $150\mu m$ long, which is $50\mu m$ shorter than the height of the part, to leave space between the tip and the wafer holding the parts while is enough to orient the insertion. The plane on the part is $260\mu m$ in width, so the pushing shoulder is $200\mu m$ in outer diameter, which is small enough not to occlude the part in top view, while at the same time big enough to prevent to the part from tilting after grasped. The height of the pushing shoulder is designed to be $150\mu m$, with the considerations of the total length of the gripper probe, the orientation after fixed to the gripper, and the feasibility of fabrication. So the entire length of the gripper probe is about $300\mu m$ plus, including the tip, the pushing shoulder and the bending corner.

3. *Gripper cantilever design*:

To make it easy to take a top view of the workspace while the gripper is above the part, the diameter of the cantilever should also be smaller than the width of plane in the part. The cantilever is designed to be $200\mu m$, the same as the pushing shoulder. And the length should be at least larger than the width of one single part, which is $500\mu m$. In practice, more parts can be viewed in the top view will make the locating

process easier and more precise, but that will mean a long cantilever, which will result in more deformation in the part during insertion.

Experiments were carried out to derive the maximum deformation the parts can withstand without being plastically deformed or damaged. Steel probe was used in the experiments to push the part in the horizontal direction, in which the part will be deformed during the grasping period. The experiment process was observed under microscope, and the part was deformed obviously by the pushing force. Measured under the microscope, when the deformation was more than $10\mu m$, there were plastic deformation and even cracks detected, which meant during the grasping period, the maximum movement of the gripper tip (d_s in Figure 3-7) was $10\mu m$. During the insertion period, the friction between the gripper tip and the wall of the part will push the probe upward, thus the cantilever of the gripper will be deformed as shown by the solid lines in Figure 3-7B.

And the bending deformation can be calculated using the following equation:

$$d_b = \frac{f_p \cdot L^3}{3 \cdot E \cdot I} \tag{3.7}$$

where h is the bending deformation at the end of the cantilever, and f_p is the pushing force (This pushing force is set to $0.5N$, which is more than double the assembly force needed). L is the length of the cantilever. $E = 400Gpa$ is the

Young's Module of tungsten, and $I = \frac{\pi \cdot r^4}{4}$ is the moment of inertia of the tungsten rod, and $r = 200\mu m$ is the radius of the tungsten rod.

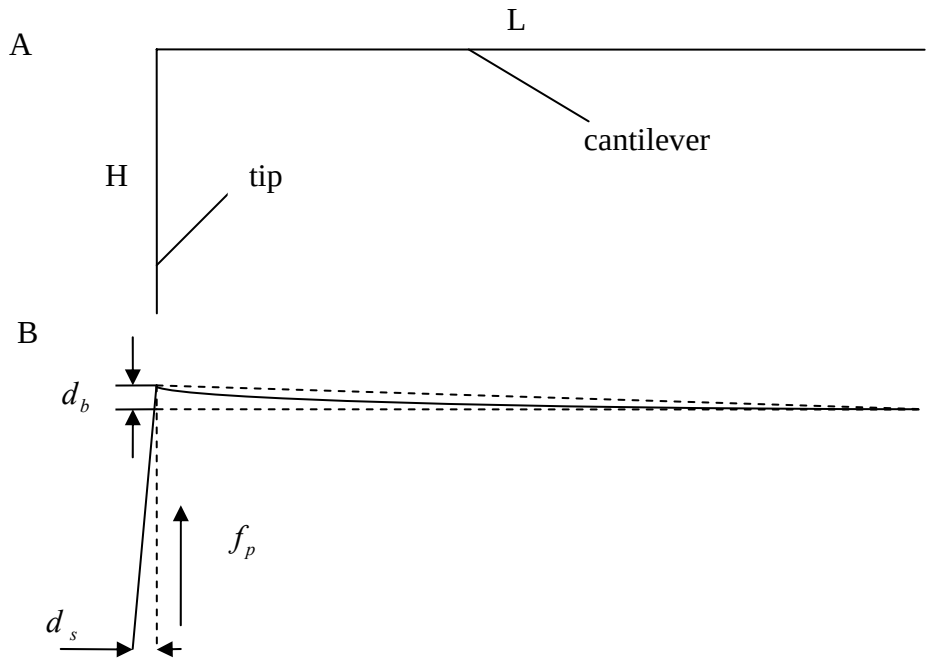

Figure 3-7 Deformation of the gripper during the insertion period.

The relationship between the length of the cantilever and the bending deformation is shown in Figure 3-8. When the cantilever is $2mm$ long, the deformation is about $2.5\mu m$ at the end, and the corresponding movement at the end of the gripper tip will be $0.5\mu m$, which is much smaller than the limitation of $10\mu m$. This is enough for 3-4 parts to be snapped in one view. Therefore the cantilever is set to $2mm$ long, which ensures both enough stiffness while inserting and enough space for top view.

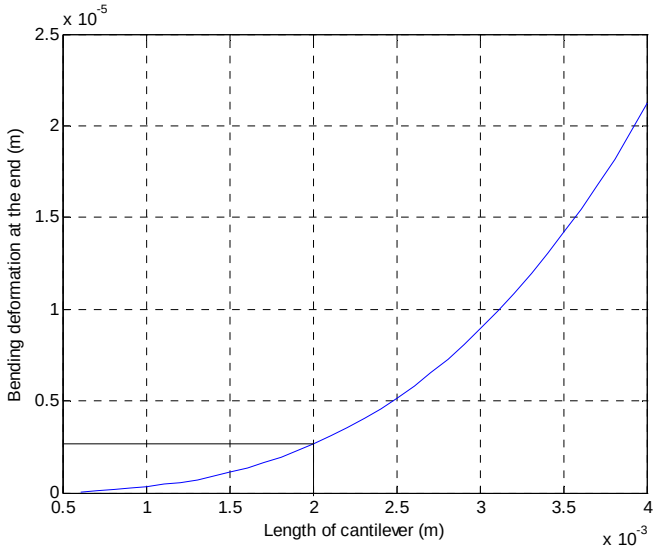

Figure 3-8 Bending deformation of tungsten rod of different dimension.

3.3.3 GRIPPER FABRICATION

The prototype of the L-shape gripper was self-made from some commercially available tungsten rod in the clean room using electrochemical etching technique (STM Tips: http://www.phys.unt.edu/stm/tips.htm). The raw tungsten rod was grasped with stainless steel tweezers (Figure 3-9), which was then fixed to a vertical moving stage with micron movement resolution for precise control of the etching depth.

1mol KOH solution was used as the strong base for the etching, and a piece of tungsten rod with diameter of $500\mu m$ was submerged into it. It took about 42 minutes at $5V$ and 12mA for the tungsten rod to be etched to $200\mu m$ in diameter. Then the etched part was bent and partially submerged into the same solution (Figure 3-9), and at the same voltage

and current, after about 10 more minutes the tungsten rod was etched to the desired dimension of 100μm in diameter.

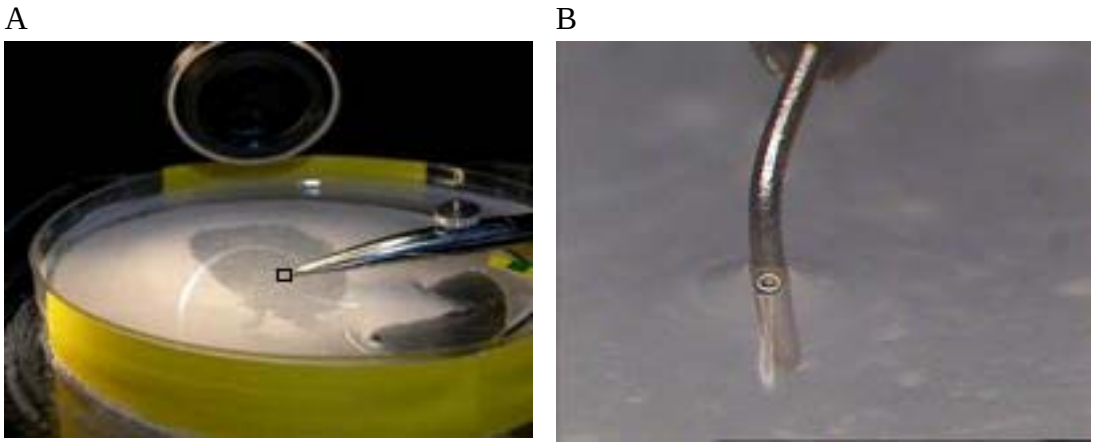

Figure 3-9 (A) Gripper fabrication setup. (B) Etching gripper probe in KOH solution.

The whole process was observed under microscope and after every few minutes the tungsten rod was taken out to measure the diameter (Figure 3-10).

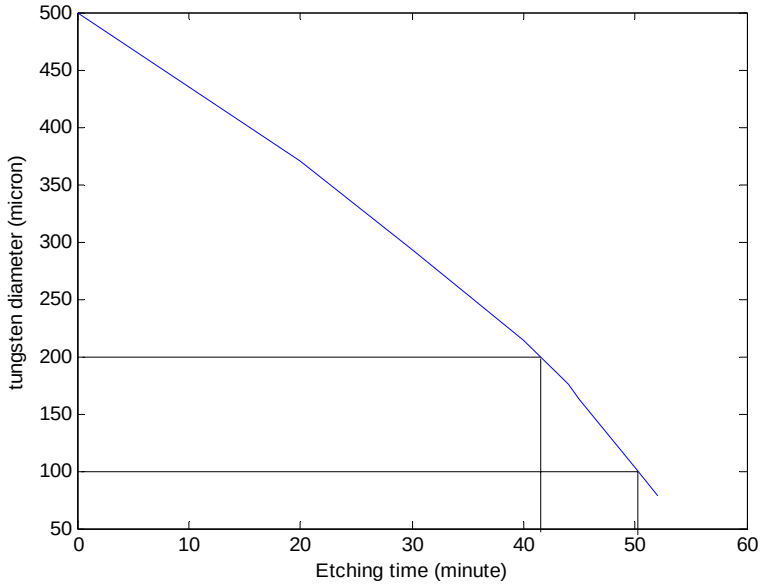

Figure 3-10 Tungsten rod etching: time and diameter.

After etching, there is slope found at the tip of the tungsten rod (Figure 3-11B), which is inevitable for electro chemical etching. In fact this is much better than a perfectly cylindrical rod, as the smaller the dimension of the tip end gives more position tolerance during the insertion period. The pushing shoulder (Figure 3-11C) with the dimension of $200(D)\times150(H)$ microns with a hole of 100 microns in diameter was fabricated using the photolithography technique, and then fixed to the tip of the tungsten rod. The finished probe gripper is shown in Figure 3-11A, and the angle between the probe and the cantilever was made a little bigger than 90 degrees to avoid the cantilever and the fixture from interfering the assembly process.

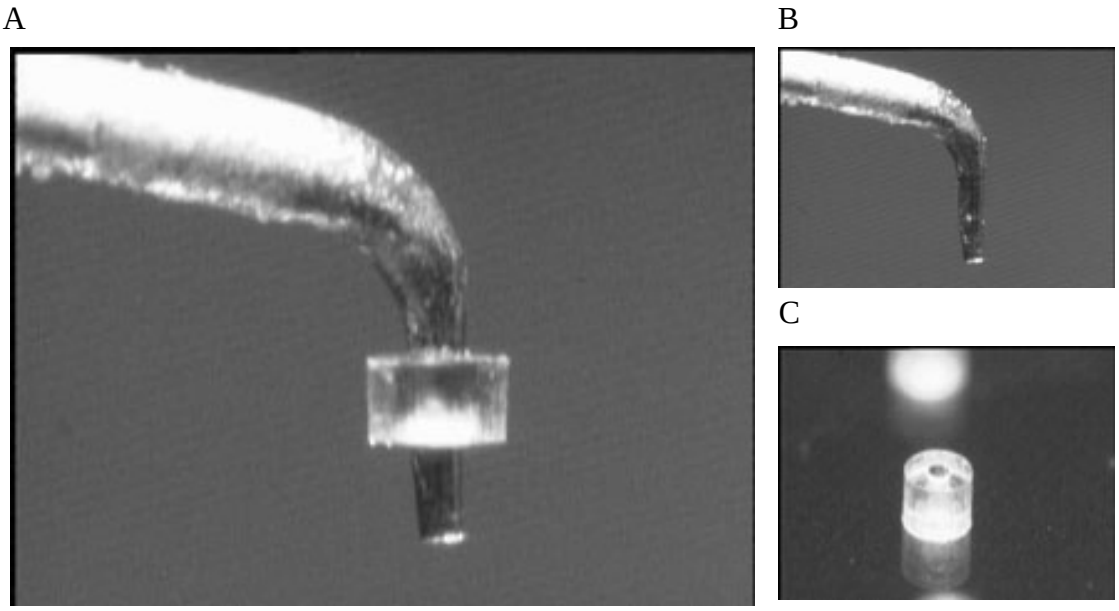

Figure 3-11 (A) Fished probe gripper. (B) Etched tungsten rod. (C) Pushing shoulder.

Experiments were carried out to evaluate the performance of the micro probe gripper. The top view was not occluded by the gripper while it was above the wafer (Figure 3-12A, B),

and there was no difficulties to guide the movement of the gripper using only the top view. The part (Figure 3-12A) as well as the zero-plate (Figure 3-12B) can be easily recognized and located. Because of the slope at the end of the gripper end, the tip can be easily inserted into the hole, and balanced and stable picking up of the part can be achieved (Figure 3-12C). The assembly force is mainly produced by the pushing shoulder, and after the assembly, the gripper can be easily released from the part by simply moving upward (Figure 3-12D). The deformation of the part during the insertion is about $2\mu m$ which is bigger than $0.5\mu m$ as calculated before, which might be caused by the deformation in the serial connection structure, but still much smaller than the limit, and will not bring any negative results.

3.4 DESIGN AND FABRICATION OF FORCE SENSOR

As mentioned in the previous sections, the proposed automatic assembly process will be accomplished with the guidance of a top view and a force feedback, i.e., the vision will control the movement in the horizontal plane to find the position to go, and the force sensor will give the information to the system to move in the vertical direction.

A survey of the commercially available micro force sensors shows that no ready-made sensor is suitable for our assembly task, for almost all the sensors were made for special tasks. Hence, a force sensor was designed and fabricated for the microassembly task.

3.4.1 FORCE SENSING TECHNIQUE

During the insertion period, the friction between the gripper tip and the hole in the part

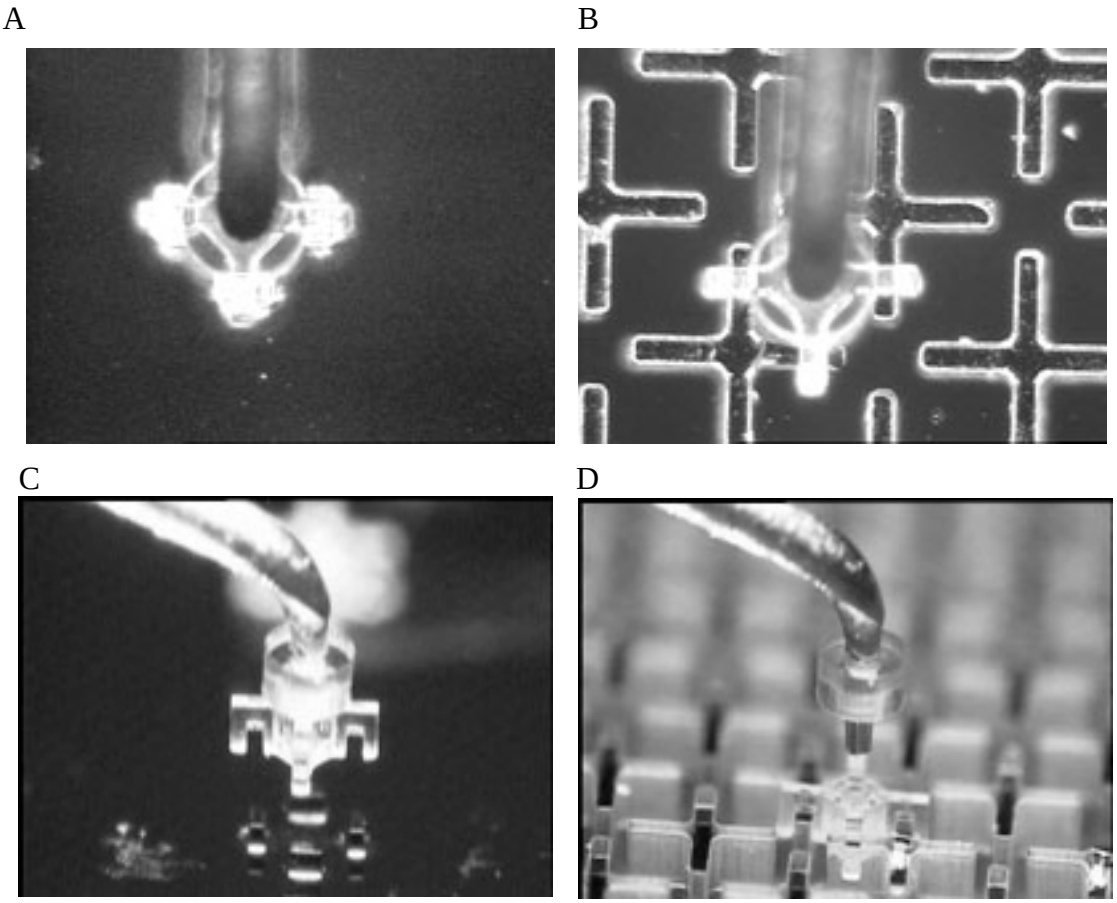

Figure 3-12 Evaluation of the performance of the micro probe gripper

(A) Top view of the gripper and part. (B) Top view of the gripper with part and zero-plate. (C) Pick up the part. (D) Release the part.

will increase continuously, as well as the bending deformation in the cantilever of the gripper. So the idea is to detect the real-time deformation of the cantilever thus get the friction. This can be achieved by attaching the micro probe gripper to the elastic element of the force sensor, and thus the elastic element of the sensor will deform correspondingly while the cantilever of the gripper was deformed. And the requirements for the proposed micro force sensor are as follows:

- *Real-time sensing*: The purpose of using the force sensor is to realize a real-time control of the movement of the gripper, and thus a real-time sensing of the gripper is essential.
- *Range*: From the analysis and calculation in previous sections, during the assembly period, the gripper should be able to produce a pushing force of $0.2N$, and so the ideal range of the sensor should be about $0.5N$.
- *Resolution*: Considering the force range and the application, the resolution should be at mN level.

After the the literature survey in chapter 2, strain gauges with piezoresistive effect were selected for the force sensing. Besides fulfilling the above listed requirements, strain gauges are also easy to mount onto the elastic element.

Micron Instruments' SS-027-013-500P (Figure 3-13) was selected to sense the deformation in the elastic element and give a voltage output that changes corresponding to the deformation. Some of its important specifications are shown in Table 3-4.

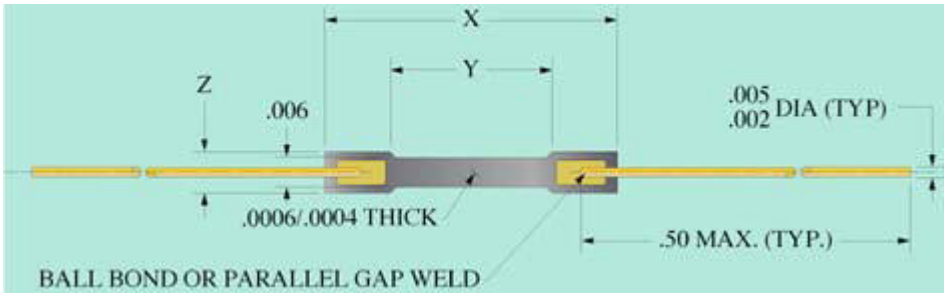

Figure 3-13 Strain gauge SS-027-013-500P.

Table 3-4 Important Specifications of SS-027-013-500P

Specifications	Value
Overall Length	6.858*mm*
Width	0.2268*mm*
Resistance	$540 \pm 50 Ohms$
Gauge Factor	150 ± 10
Operating Strain	$\pm 2000 \mu inch / inch$ ($3000 \mu inch / inch$ max.)

3.4.2 SENSOR BODY DESIGN

The sensor body consists of three main segments as shown in Figure 3-14.

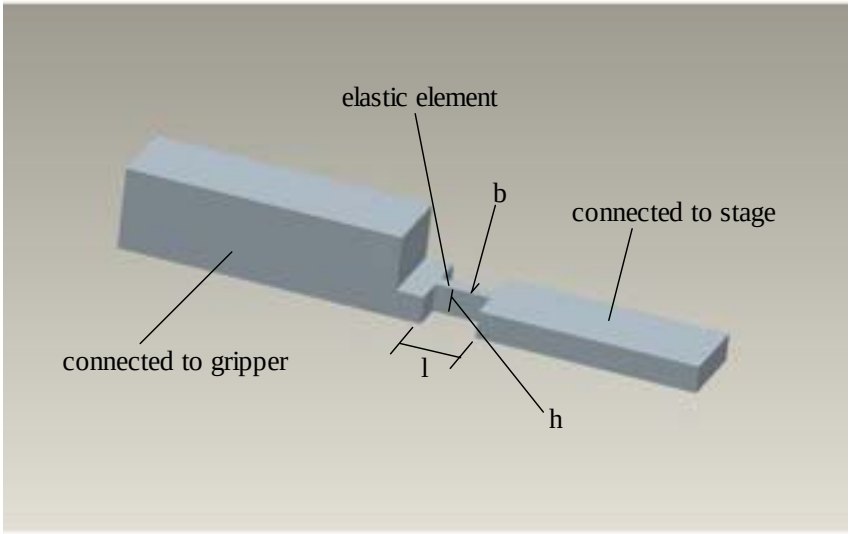

Figure 3-14 Sensor body.

The segment marked as “Connected to gripper” is designed for connecting to a gripper clamper, which is used for a transition between the micro probe gripper and the correspondingly larger force sensor. The segment marked as “Elastic element” is for attaching the strain gauges, which is the main part of the sensor. The segment marked as “Connected to stage” is designed for connecting to the stage which moves in the vertical direction.

Using such a sensor, the force that the sensor is supposed to measure will act at one end of the cantilever, which contains the micro probe gripper, the gripper clamper, and part of the sensor body, while the strain gauges will be attached to the other end of the cantilever where the deflection, and hence the strain, has the maximum value. In this way, the sensitivity of the sensor will be increased without reducing the stiffness of the cantilever.

Elastic element is the key part in force sensor, for it converts the mechanical quantity, into deflection or strain which can be transformed using the strain gauges attached on it to an elastic signal. The design of elastic element is a trade-off between stiffness and sensitivity, i.e., the more sensitive the force sensor is; the less stiff the structure will be.

In the following analysis, the micro probe gripper, the gripper clamper, the segment of the sensor body used to connect to the clamper and the elastic element is simplified as a cantilever as shown in Figure 3-15.

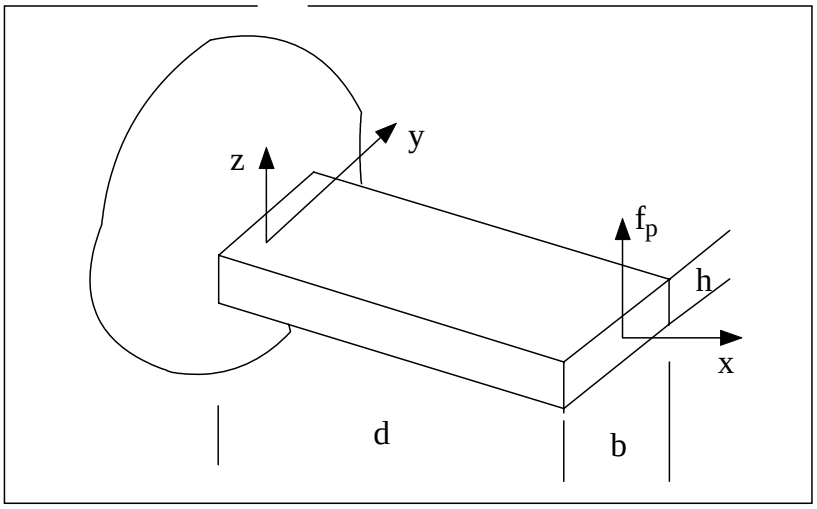

Figure 3-15 Cantilever deformation.

A concentrated force loaded at the free end of the beam, and it has a rectangular cross section just as the elastic element, and simulation was carried out to insure that the simplified model has the same property as the real condition.

The maximum bending moment M occurred at the supporting end of the cantilever which is given by:

$$M = f_p d \tag{3.8}$$

where f_p is the loading force from the micro probe gripper, and d is the length of the cantilever.

According to theories of mechanics of material, strain ε is given by:

$$\varepsilon = \frac{My}{EI_z} \tag{3.9}$$

where y is the position of the neutral axis, E is the elastic modulus and I_z is the area moment of inertia with reference to the neutral axis. E, also Young's Modulus, indicates the stiffness of material within the elastic range. The material of the sensor body was chosen to be aluminum, which has a lower stiffness than the micro probe gripper, thus allowing a higher sensitivity of the force sensor, so $E = 73.1Gpa$. I_z is solely decided by the shape of the cross section. In our case, strain gauges will be glued symmetrically on both of the surfaces, so the position of neutral axis is $y = h/2$, and for rectangular cross section, the area moment of inertia is

$$I_z = \frac{b \cdot h^3}{12} \tag{3.10}$$

where b and h are the dimensions of the cantilever as shown in Figure 3-15, the strain can be obtained as:

$$\varepsilon = \frac{6 f_p d}{E h^2 b} \tag{3.11}$$

To simplify the problem, the gripper clamper is taken as a rigid body, and so the deflection of the free end can be estimated as:

$$\delta = \frac{ld}{\rho} \tag{3.12}$$

where l is the length of the elastic element and ρ is the radius of curvature of the elastic element. ρ is given by:

$$\rho = \frac{EI_z}{M} \tag{3.13}$$

Then the deflection of the free end can be derived as:

$$\delta = \frac{12 f_p l d}{E b h^3} \tag{3.14}$$

For l affects only the stiffness of the cantilever, and independent of any other dimensions or properties of the cantilever, it is chosen to be $3mm$ which is just enough for the strain gauges. b was chosen to be $3mm$, which insures enough stiffness while allows high sensitivity. Considering that microscope is to be mounted above the cantilever for the top view, the length of the cantilever should be more than $60mm$. And the relation between the strain and the height of the cantilever at different cantilever length of the cantilever was calculated (Figure 3-16).

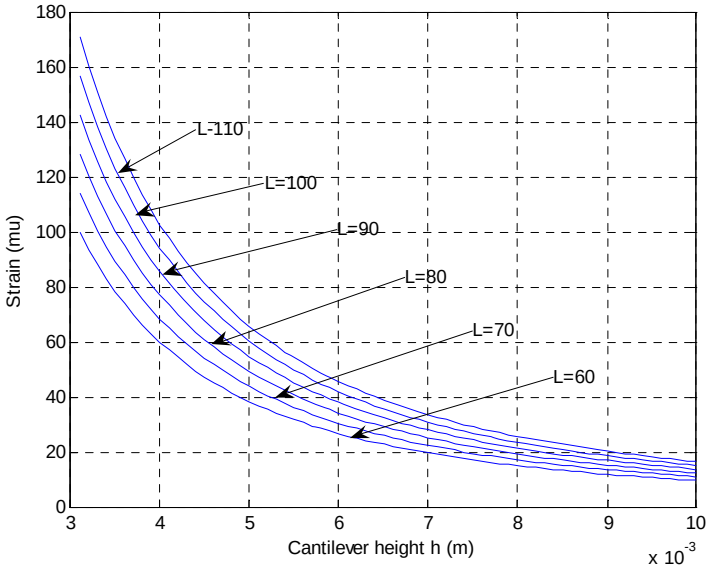

Figure 3-16 Calculation of relation between ε and h.

And the relation between deflection and height at different cantilever length is shown in Figure 3-17.

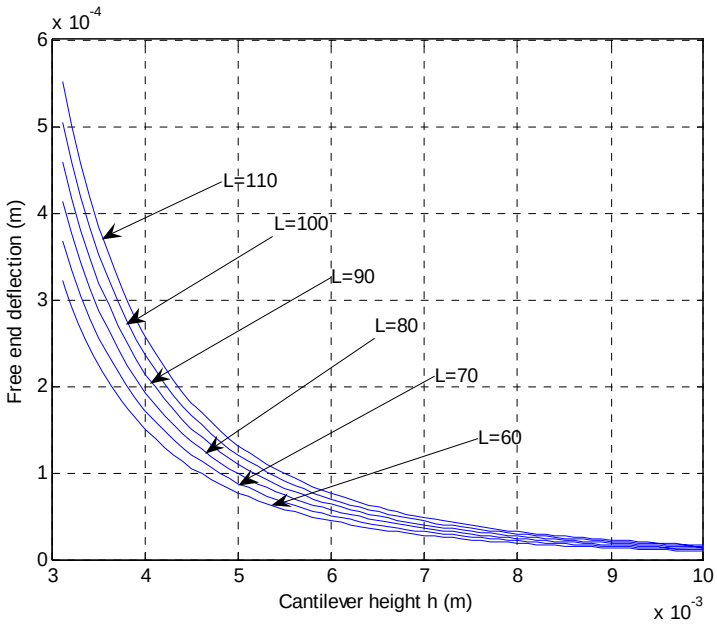

Figure 3-17 Calculation of relation between δ and h.

As analyzed from previous sections that the sliding distance of the gripper tip should be less than $200\mu m$, the deflection should be smaller than $200\mu m$. And also to insure the sensitivity, the strain should be greater than 30μ. Finally d was chosen to be $100mm$ and h was chosen to be $5mm$.

3.4.3 SENSOR FABRICATION AND SENSING MODULE CONFIGURATION

The integration of the strain gauge sensor requires great care: when bonding semiconductor strain gauges, attention must be given to each process step as the quality of the finished sensor is totally dependent upon the correct process (Vishay: http://www.vishay.com/brands/measurements_group/guide/ib/b129/129index.htm). The

following steps were taken during the fabrication of the sensor, and for the small dimension of the strain gauges, the bonding process was finished under microscope.

1. The top and bottom surface of the elastic element where the strain gauges are placed were accurately polished and cleaned.
2. Gauge-location layout lines were marked in the centre area of the elastic element where the strain measurement is to be made for accurately relocating and orienting the strain gauges.
3. A layer of strain gauge adhesive, which is epoxy glue, was applied the elastic element area, and this is for precoat as well as electrical isolation of the strain gauges as regards the sensor body.
4. The cured precoat surface was then abraded with pumice powder, which was previously moistened with conditioner, to achieve an ideal surface for integrating the strain gauges.
5. Bonding the strain gauges. The area in both of the top and bottom side of the elastic element to bond the gauges was first coated with epoxy glue, which is the same as used for precoat, and then the gauges were merely placed into position; the attaching was achieved by the capillary force between the gauge and the precoat, and no clamping was used ao as not to damage the gauges.

The next step after bonding the strain gauge is the realization of the electrical connection. Micron’s bondable terminals MST 125 were used for connecting the strain gauges leads to larger instrumentation leads. The epoxy glass layer of the terminals insures superior election insulation, and the solder tap provides an anchor and thermal barrier for both sets

of leads. The two strain gauges attached at the top and bottom surfaces of the elastic element form a half Wheatstone bridge, with one strain gauge of the pair measuring the compression and the other one measuring the tension. This type of configuration has high sensitivity to bending strain, ability to reject to axial strain and can compensate for temperature effects.

The output voltage from the strain gauges can be calculated from:

$$V_o = 0.25 \cdot N \cdot GF \cdot \varepsilon \cdot V_e \tag{3.15}$$

where $N = 2$ is the number of active arms of the Wheatstone bridge, i.e., the number of strain gauges used in the bridge circuit, $GF = 155$ is the gauge factor, ε is the strain acting on the strain gauges, and V_e is the excitation voltage, which is usually smaller than $10V$. It is set to be $5V$ in our experiments.

From Equ.(3.15), the maximum voltage output that may exist in our experiment will be $27.125mV$ when a maximum strain of $70\mu strain$ is acted on it as calculated in previous section.

Signal processing is accomplished by using TML's one channel dynamic strainmeter DC-92D, which has the main functions of gauge bridge, auto-balancing, signal filter and signal amplification. Some of its important specifications are shown in Table 3-5.

3.5 INTEGRATION AND CHARACTERIZATION

The integration of the sensor to the gripper was achieved by using a stainless steel gripper clamper, and the finished gripper with force sensing module is shown in Figure 3-18.

Table 3-5 Important specifications of TML DC-92D.

Specifications	Value
Gauge resistance	$60 \sim 1000\,\Omega$
Bridge excitation	DC 0.5, 1, 2, 2.5, 5, $10\,V$
Output	Voltage $\pm 10\ V$ to $5\,k\Omega$ load
Range adjuster	Gainx (10000, 5000, 2000, 1000, 500, 200)
Maximum measuring	50000×10^{-6} strain, 50 mV (Voltage Input)

Calibration of the force sensing module was achieved by pushing the tungsten tip grasped by the gripper clamper against an electrical balance (Model AB204-S, Mettler Toledo, New York, USA – full scale $200\,g$, accuracy $0.01g$). By doing so, the relation of the sensor output and the applied force is obtained (Figure 3-19).

The calibration was done by pushing the free end of the cantilever down onto the electrical balance step by step until the force reached about $0.7N$, which is more than needed, and then lifted the cantilever until the force returned to zero. The results showed the good linearity of the strain gauge sensor whether the cantilever is horizontal (Figure 3-19A) or there is an angle between the cantilever and the horizontal (Figure 3-19B). When there is an angle, hysteresis was observed during the lifting period, but the output voltage still

returned to zero while the applied force was zero, so this will not affect the use of the force sensor.

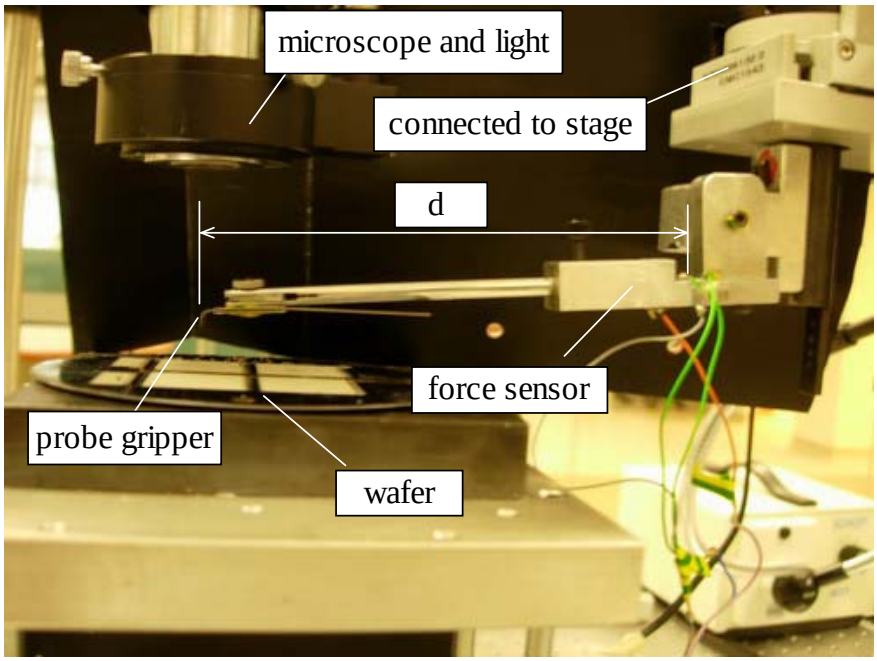

Figure 3-18 Integrated gripper and force sensing module.

The result suggests that a cantilever fixed horizontally guarantees better linearity of the sensor, which means a more stable dynamics of the system.

And the corresponding resolution of the force sensor was calculated as follows:

The sensor signal was read through the Servo-To-Go card, which has a 13 bit resolution with $\pm 10V$ full scale input, so the bits the A/D can convert is:

$$2^{13} bits / 20V = 409.6 bits / V \tag{3.16}$$

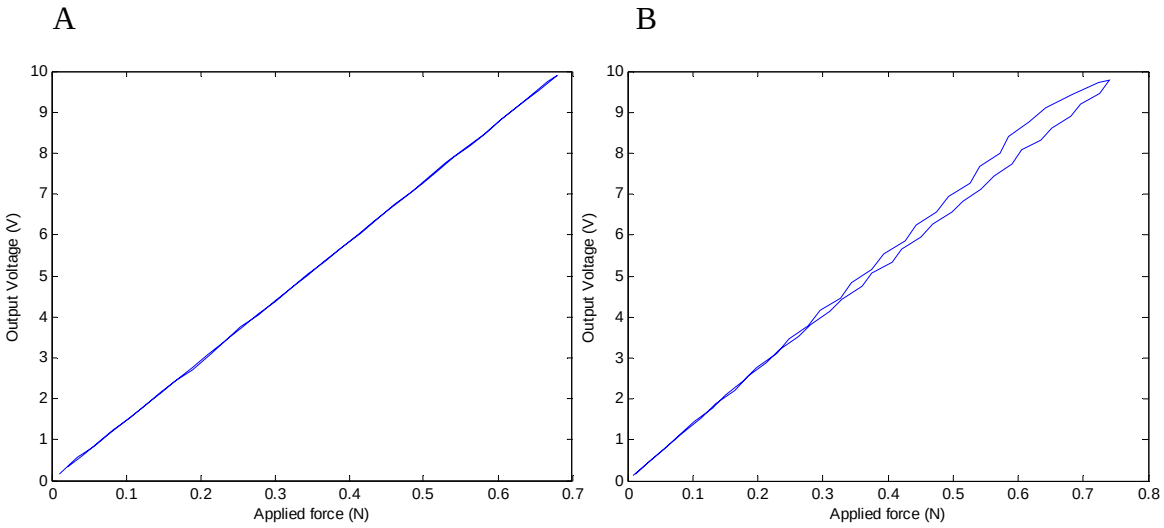

Figure 3-19 Calibration by electrical balance: force generated by gripper against output signal (amplified and filtered) of semiconductor strain gauge bridge

Cantilever is horizontal. (B) Cantilever is 10 degrees angle to horizon.

And from the calibration process, we get the relation between input force and output voltage, and $0.68N$ input gives $10V$ output, which equals to

$$10V \times 409.6bits/V = 4096bits \tag{3.17}$$

output. And thus the amount of force can be measured by 1 bit is

$$0.68N/4096bit = 0.166mN/bit \tag{3.18}$$

Thus the force sensor has a resolution of $0.166mN/bit$.

The idle and loaded outputs of the force sensor, after conditioned by the strainmeter, are shown in Figure 3-20 and Figure 3-21. Under both conditions, the maximum deviation of the output voltage from the sensor is under $0.05V$, and the standard deviation of this

filtered signal is $0.015V$. As is typical of semiconductor strain gauges, $1/f$ noise is present in the sensor output at low frequencies.

3.6 CONCLUSION

A force sensor integrated micro probe gripper was designed and the prototype was fabricated in the clean room environment. The micro probe gripper was made by using electro chemical technique from some commercial available tungsten rod. The dimension is about 100 microns in diameter at the probe tip, and 200 microns in diameter at the

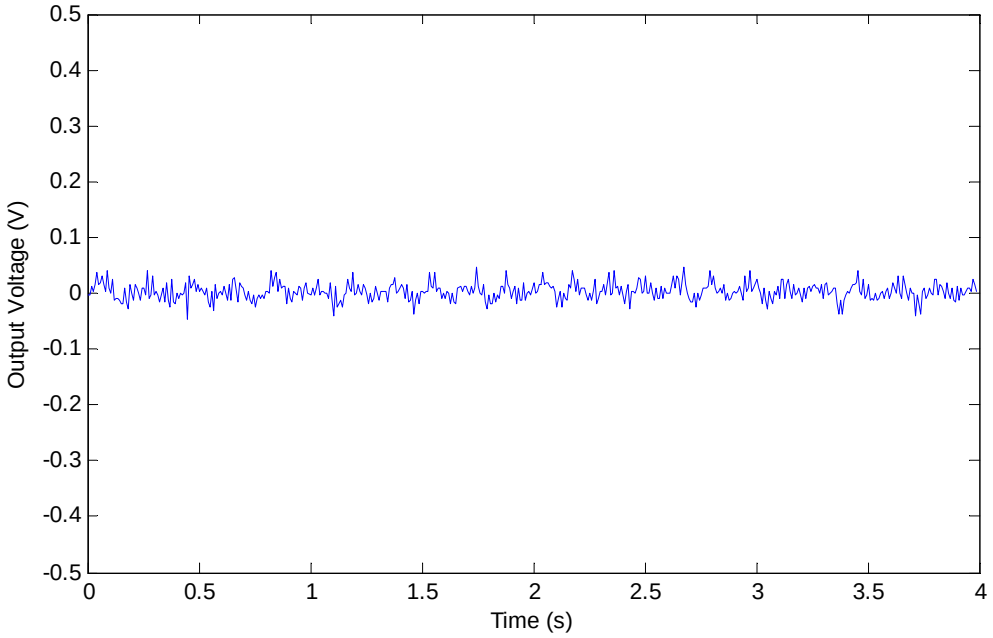

Figure 3-20 Sensor noise and drift when idle.

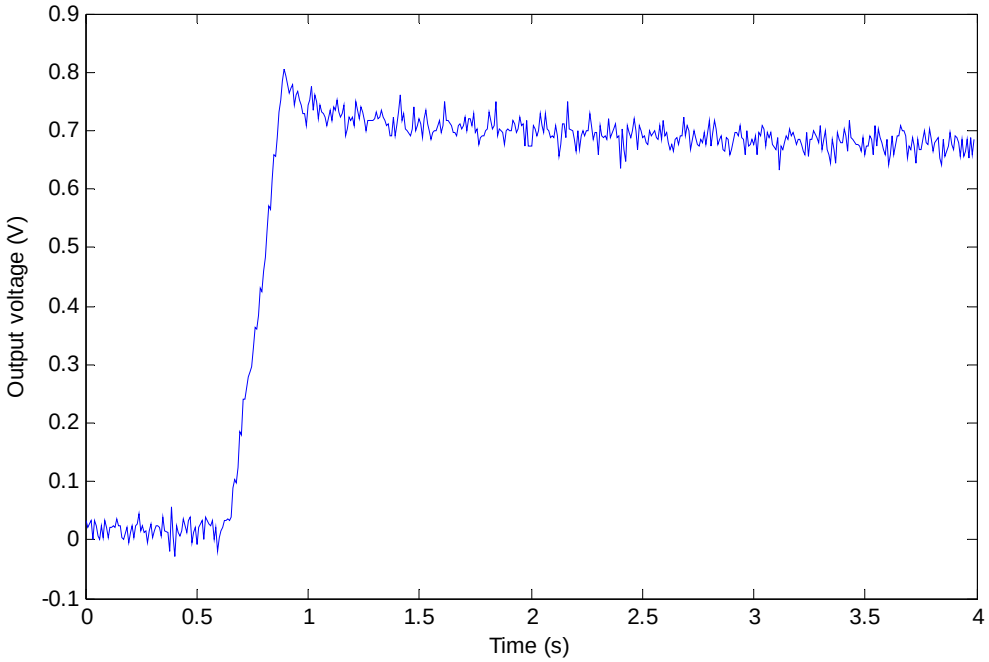

Figure 3-21 Sensor noise and drift when loaded.

cantilever part. A polymer pushing shoulder was fabricated and fixed to the gripper tip to accomplish the assembling work.

The force sensor body was made by conventional tooling technique from aluminum, and a pair of semiconductor strain gauges was adopted in the force sensing for higher sensitivity and temperature compensation. The calibration results shows good linearity of the force sensor in the range of 0 ~ 0.7 Newton, and the resolution can reach sub-milli Newton level. Typical noise are present in the sensor, but since the amplitude is less than 1/100 of the value we need, it will not disturb the assembly process.

The force sensing integrated micro probe gripper is well suited for the redesigned micro parts, and a real-time force control of the assembly process can be realized using the modified hardware.

Chapter 4

Automatic assembly system

4.1 INTRODUCTION

The objective of this project is to realize an automatic assembly of 3D scaffold from micro parts, which have the dimension of several hundred of microns. Different from assembly tasks in macroworld, microassembly poses new challenges and problems in the fabrication of microscopic components, the development of micro tools, hardware, control strategy and software of the robotic systems. Microassembly has been investigated in the past decades and is still the object of extensive research. Some main issues in microassembly are shown in Table 4-1 (Böhringer et al, 1999), (Grutzeck and Kiesewetter, 2002).

To accomplish the automatic scaffold assembly task in our project, the micro parts needed to be transferred from the original wafer to the target wafer controlled by a supervisory system using the combined information of a vision and a force feedback from the working space. Hence, a desktop assembly system was built for our microassembly task, which comprised mainly of a precision desktop workstation (hardware) and supervisory system software.

Table 4-1 Main issues in microassembly.

	Teleoperated handling of miniaturized parts	Teleoperated assembly of miniaturized parts	Teleoperated assembly of a case products	Automatic handling of miniaturized parts	Automatic assembly of miniaturized parts	Automatic assembly of a case products
Microscope system	X	X	X	X	X	X
Precision positioning	X	X	X	X	X	X
Handling tools	X	X	X	X	X	X
Master controllers	X	X	X			
Control system	X	X	X	X	X	X
Environmental control	X	X	X	X	X	X
Force sensing	X	X	X	X	X	X
Signal conditioning	X	X	X	X	X	X
Feeding system		X	X		X	X
Precision connection tools		X	X		X	X
Product related tools			X			X
Position sensing				X	X	X
Automation system				X	X	X
Advanced automation system					X	X

4.2 PRECISION DESKTOP WORKSTATION

From the above listed requirements for the microassembly system for our scaffold assembly task, the dedicated desktop workstation (Figure 4-1) contains three modules as follows:

1. *Positioning module*: The positioning module has five degrees of freedom (DOF) which is realized through three translation stage, one vertical micropositioning stage, and one rotation stage.
2. *Sensing module*: The sensing module contains the force sensing module as developed in last chapter and a vision sensing module, which contains two microscopes, 2

lighting sources, two CCD cameras, and one image grab card, image processing software.

3. *Micro probe gripper*: As described in last chapter, the gripper is made from fine tungsten rod. It has an extremely fine tip (can be smaller than 100 microns) and meanwhile sustains a relatively high bending force so it can provide enough pushing force to parts and minimize vision occlusion at the same time.

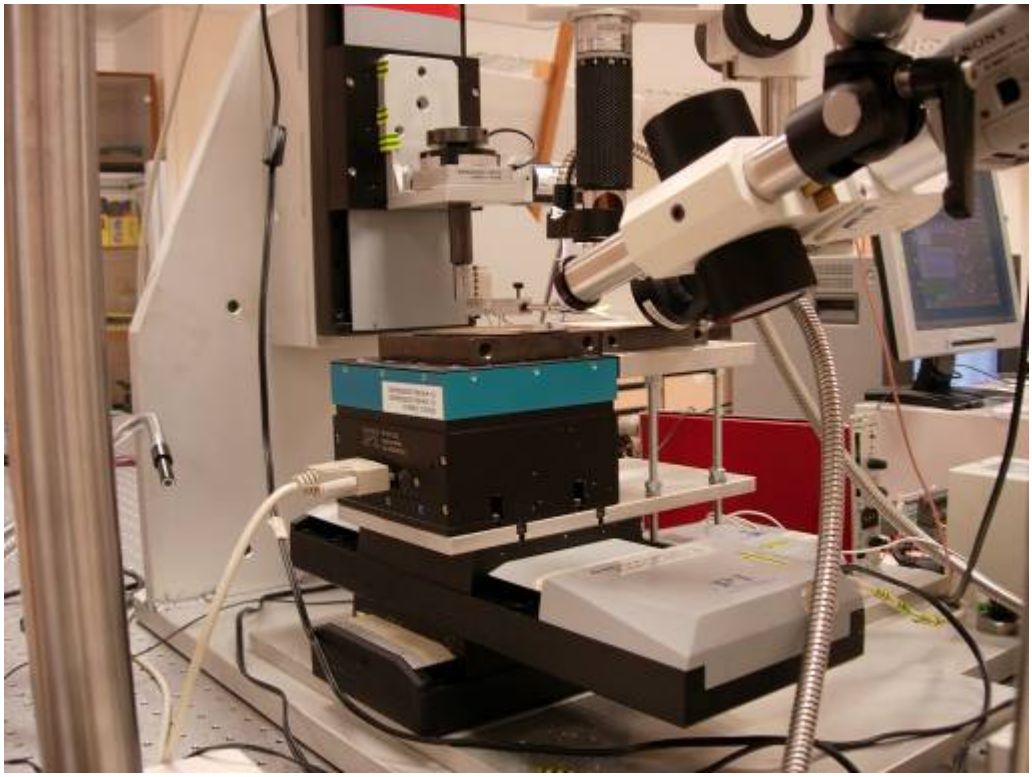

Figure 4-1 Precision desktop workstation.

An assembled scaffold for practice use may contain at least hundreds of micro parts distributed in several layers, and building such a structure needs a system with multiple DOF and can move in several directions. To fulfill this purpose, a five degree-of-freedom desktop workstation is adopted, and the configuration is shown in Figure 4-1.

Two translation stages were fixed together to work as the conveyer in x-y plane. Physik Instrumente (PI)'s low-profile, high-resolution translation stages M-511.DD were adopted, and some of its main specifications are shown in Table 4-2.

Table 4-2 Main specifications of M-511.DD.

Specifications	Value
Travel range	102 mm
Design resolution	0.1 μm
Min. incremental motion	0.1 μm
Accuracy per 50 mm	0.2 μm
Max. velocity	50 mm / sec
Encoder resolution	0.1 μm
Max. normal load capacity	100 kg
Max. push/pull force	80 N

The transfer of parts from its original wafer to the target wafer and the assembling of parts to different position in one layer are realized by these two stages. The specifications of this precision stage allow a fast transfer of the parts and at the same time ensures enough accuracy for allocating the parts.

One of PI's vertical micropositioning stages (Model M-501.1PD, PI, Germany – full range 12.5 mm, resolution 0.008 μm) was mounted on top of the translation stage working as a conveyer as well as an assembly platform. There is a home-made specially designed connector fixed between the vertical stage and the translation stage under it. A height-

adjustable platform was fixed above the connector parallel to and side by side with the vertical stage. Thus, during assembly, the part magazine which is the original wafer holding the parts will be placed on the platform in the focus plane of the top-view microscope, and the target wafer will be placed on top of the vertical stage with the top layer also in the focus plane of the microscope. And after each layer of scaffold is assembled, the vertical stage will move down a distance such that the top layer of the scaffold is always in the focal plane of the microscope.

The force sensing module with the integrated micro probe gripper will be mounted to a rotation stage (Model M-037.DG, PI, Germany – rotation range continuous, resolution 0.59 μrad), which is used only in the initialization stage to adjust the angle of the gripper cantilever and ensure that it is parallel to the columns of the parts.

The rotation stage then is fixed to another vertically placed PI's translation stage (Model M-511.DDB), which has the same specifications as the other two translation stage M-511.DD except for an integrated brake to stop the stage from sliding downward due to gravity while the power is off. The vertical will work as the actuator of the gripper to realize all the movement of the gripper in the z direction.

A PI's C-842 multi-channel controller is used to control the five stages. Due to the limited channels of C-842 (4 channels), after initialization, the rotary stage has to be disconnected from the controller to free a channel for the vertical stage. C-842 is based on a multi-processor architecture. It includes a fast DSP motion-control chip set (providing trajectory

generation and closed-loop digital servo control based on position information from the encoders) and a host processor for communication and command handling. It has *S*-curve profile generation which enables smooth velocity changes and a 32-bit PID servo-control.

Two Zeiss microscopes with a long working distance of 48mm are used in this project to provide both side view and top view. Both of them have a Sony digital camera with 1/3-inch CCD replacing the binocular eyepieces. The side view microscope is used only for initial calibration and after that only the top view provides constant vision information during microassembly process. Signal from the top view microscope is transmitted to a Matrox Meteor II graphics card, and then to the computer for further processing.

The micro probe gripper and the force sensing module are just as described in last chapter. And the whole workstation was placed on an anti-vibration table to avoiding any disturbance from the environment.

4.3 COMPUTER CONTROL SOFTWARE

4.3.1 CONTROL INTERFACE

Communications between the software and the desktop workstation are through several cards for different part. Controlling of the stages movement is through PI's C-842 multi-channel controller. Reading force signal for the sensor is through a Servo-To-Go card. And image from the microscope is transmitted through Matrox Meteor II graphics card. VenturCom's Real-time Extension (RTX) subsystem was added to Windows 2000 to improve its real-time capabilities, which enables the instant communication between the

PC and the force sensor. Matrox Imaging Library (MIL) is used to program the graphics card. A control interface written in Microsoft Visual C++ is shown in Figure 4-2.

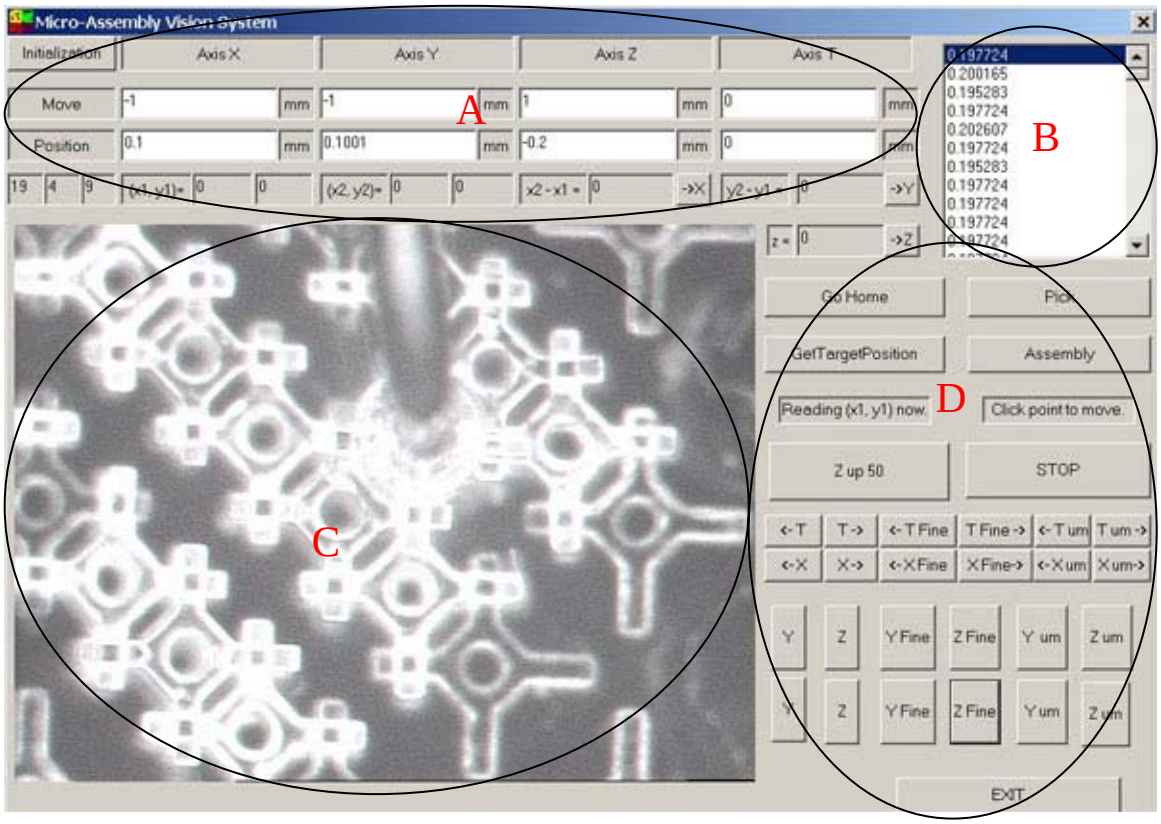

Figure 4-2 Control interface: (A) position and movement of each stage.

(B) Reading from force sensor. (C) Top-view of work space. (D) Control buttons.

Through the computer control interface, the user can realize a full control of the assembly process. The operator uses the top view of the workspace to locate the parts in the wafer, and then manipulates the movement of each stage. At the same time, the position and movement of the stage can be read from the interface as well as the reading from the force sensor.

4.3.2 ADVANTAGES OF FORCE CONTROL FOR MICROASSEMBLY

The objective of this project is to realize an automatic assembly of the tissue engineering scaffold, and the advantage of this automatic assembly compared to the human operator teleoperated assembly is its high efficiency, which includes high velocity and high yield.

Considering the assembly process, the movement of the gripper includes moving parallel to the assembly platform and moving vertically to the platform to pick the part and to assemble the part. The parallel movement of the gripper is totally contact free, and so the gripper can move in a high speed. But during the vertical movement, the gripper will move down to grasp the part and then move down to assembly the part, and these movements involve the transition from free movement to contact and then to constrained movement with the constraints changing constantly. The force characteristics during the insertion at a constant velocity are shown Figure 4-3.

The gripper finished the insertion at a constant velocity in about 0.5 second, which is ideal for the assembly. There is no outstanding impact force observed during the contact transition period, and so it is not necessary to implement the contact transition control. But there are some problems with the process as follows:

- During the insertion experiment, a force threshold was set, i.e. the stage will stop moving when the output from the sensor reaches the threshold. This threshold was obtained from experiments and meant successful grasping of the part. The stage was supposed to stop when the force reaches $200mN$, but it can be seen from the figure

that it stopped until the value reached almost $400mN$. The overshoot is quite big compared to the threshold and this may cause damage of the gripper as well as the micro part.

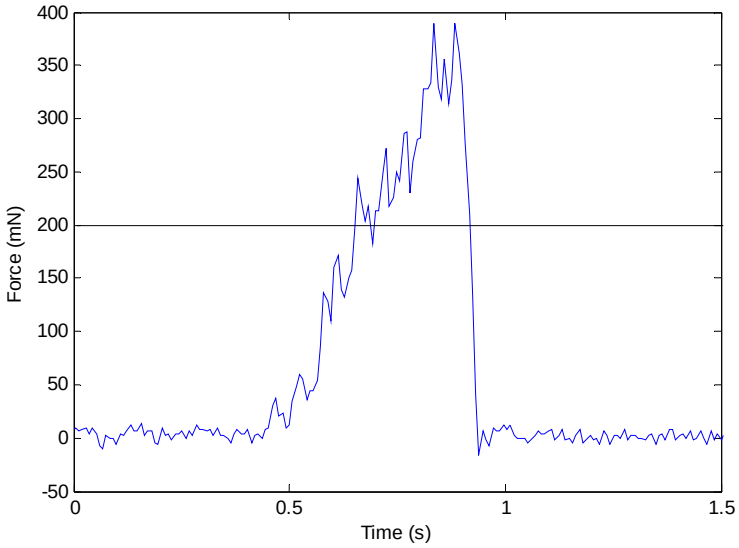

Figure 4-3 Force characteristics during insertion at constant velocity.

- The force changes rapidly during the period, especially the last steps during the insertion, which may cause the scaffold to be vibrating and unstable.

To solve the above listed problems, and protect the thin gripper and the fragile micro parts, a real-time control of the assembly force must be implemented. To date, most of the force controls in micro world are mainly devoted to grasping force control (Tortonese et al, 1991), (Ge Yang et al, 2001), (Eisinberg et al, 2001), (Deok-Ho Kim et al), (Park and Moon, 2003). Assembly force or the force control in inserting action is rarely reported. One difficulty of control inserting force is to embed force sensors between arm and

gripper. Micro assembly tasks intrinsically demand a high positioning accuracy, which not only means high precision stages but also high stiffness of the arms, joints and grippers. High resolution force sensors normally have delicate and, in most cases, fragile elastic elements. If these sensors can be and is embedded into the moving part of the assembly system, the systems positioning accuracy and robustness will largely be reduced. A force sensor with both high stiffness and high resolution is still quite a challenge. So far most of the inserting tasks were done in a teleportation fashion based on vision information only (Ge Yang et al, 2003), (Skidmore et al, 2003) (Nikolai et al, 2004). But as analyzed in Chapter 1, a vision guided microassembly process is very time consuming and inaccurate.

Typically there are two methods adopted for real-time control: position-based force control and explicit force control. But a pure position-based assembly approach is not suitable for dealing with interaction forces that constantly changes during assembly compared to an explicit force control for the two reasons.

First, in a short-range part handling and assembly operation, pure position-based method cannot directly control the interaction force between the micromanipulator and a part, particularly when the force has an uneven changing profile as the one observed in our microassembly process (Figure 4-3). But with explicit force control, in which the input signal and the measured signal are direct representations of magnitudes of force, the force profile can be controlled instantly by limiting the magnitude of the input signal.

Second, since different parts may have different mechanical properties, thus a method of position-based force control may not produce consistent results in repetitive assembly tasks, and insertion fundamentally depends on force rather than on position. In preliminary experiments, we compared the insertion depth and insertion force of assembled microparts when the micropart was inserted in 1 micrometer steps. A part was considered as assembled when the lower layer came with the assembled part. We found that the reproducibility, measured as the standard deviation divided by 20, which is the number of samples, was of 10% for the insertion depth and only 5% for the force (Figure 4-4, 4-5). This suggests that the force is a more appropriate control parameter than the distance. Furthermore, controlling force may prevent breaking parts, as too large tension will be detected by a force sensor in contrast to distance measurement.

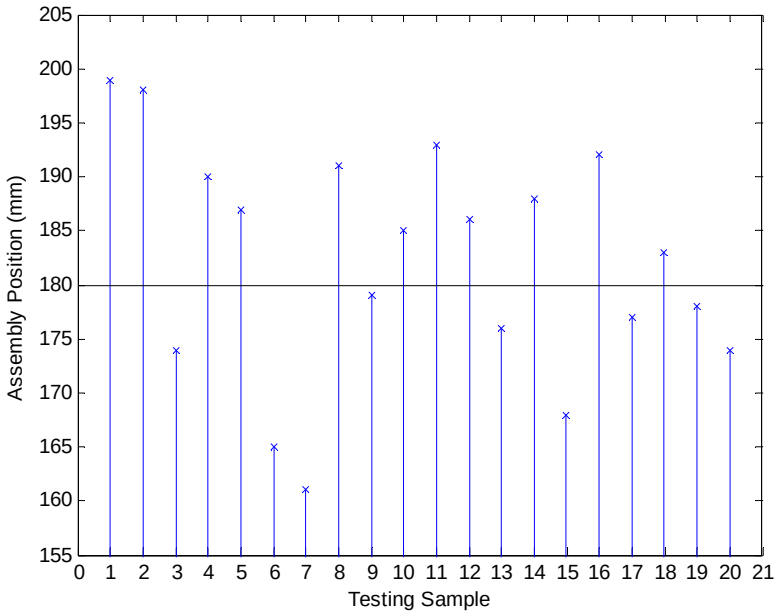

Figure 4-4 Depth of successful inserted parts.

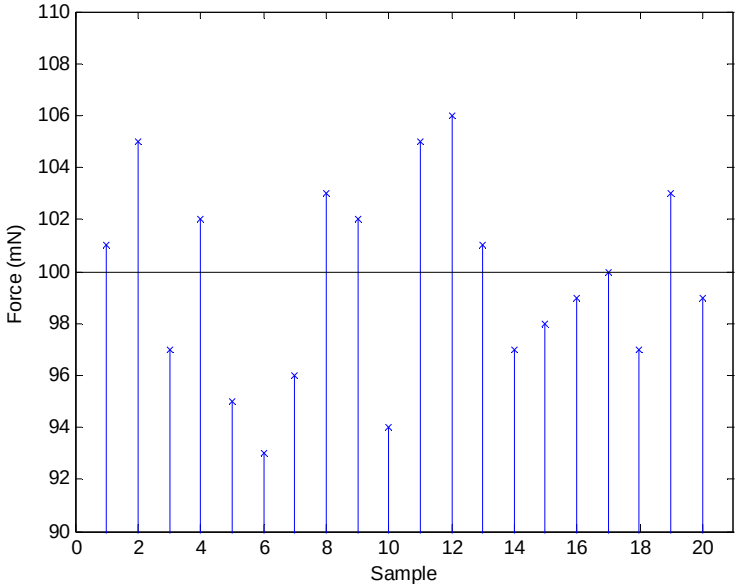

Figure 4-5 Force of successful inserted parts.

4.3.3 LIMITATION OF COMMERCIAL ACTUATOR AND THE OPERATING ENVIRONMENT

From the description of the desktop workstation, the micro probe gripper was mounted on a translation stage in z direction, which works as the actuator of the gripper. So the real-time force control will be realized through this commercial actuator (PI, Model M-511.DDB). And there are certain limitations of the commercial actuator to implementing the real-time force control.

First, the stage can run at four trajectory profile modes: s-curve point to point, trapezoidal point to point, velocity contouring and electronic gear. Each mode has its own applicable condition, and trapezoidal point to point (Figure 4-6) was chosen in our experiment for

real-time control and fast response. In the trapezoidal point to point profile mode the host specifies a destination position, a maximum velocity and the acceleration. The trajectory is executed by accelerating at the commanded acceleration to the maximum velocity where it coasts until decelerating such that the destination position is reached with the axis at rest (zero velocity). If it is not possible to reach the maximum velocity (because deceleration must begin) then the velocity profile will have no “coasting” phase. The acceleration rate is the same as the deceleration rate. And this means that the stage cannot be real-timed controlled by sending force signal directly to it, there must be a conversion from the output force signal of the force sensor to position signal which can feed to the actuator.

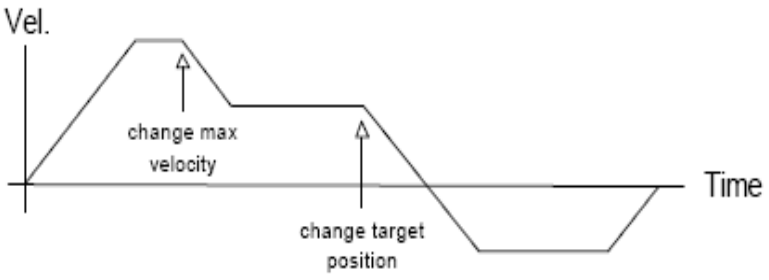

Figure 4-6 Complex trapezoidal mode motion

Second, experiments were done to test the response rate of the system. The test was implemented by feeding simple harmonic motion signal (Figure 4-7) with the amplitude of $0.5mm$, which is the distance the stage will go in the assembly task. Response of the motion and the force was observed and recorded to evaluate the capacity of the system.

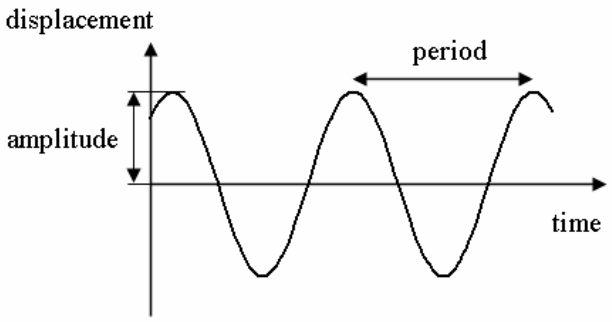

Figure 4-7 Simple harmonic motion signal.

The capacity of the control software was first tested by inputting simple harmonic signal with a period of $1\sec$. It is found that the stage can follow the input with no problem when the sampling rate is set up to $5m\sec$. And when the rate exceeds $5m\sec$, the stage started vibrating around the original position. A frequency of $200Hz$ is enough for our real-time control.

The force response from the sensor was also tested using the same input as used for testing the stages, and the results are shown in Figure 4-8. When the input signal period is longer than $0.6s$ (Figure 4-8A), the force can follow perfectly, and when the period becomes shorter ($0.3s$ for Figure 4-8B and $0.15s$ for Figure 4-8C) until $0.15s$, the force can still follow the input signal, despite some roughness. And when the period exceeds $0.15s$, the force cannot reach the set amplitude.

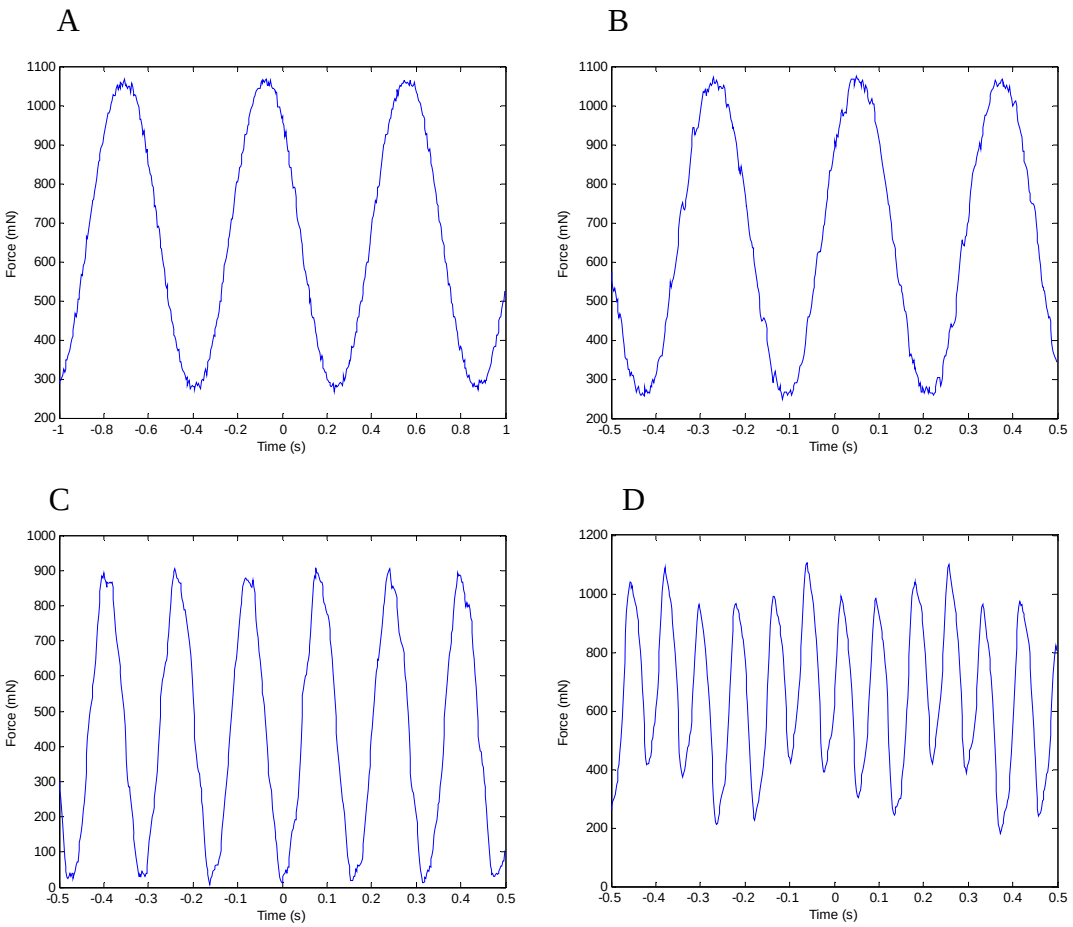

Figure 4-8 Force response to simple harmonic signal input.

4.3.4 FORCE-BASED ADMITTANCE CONTROL

The system to be controlled includes the commercial stage, some connectors and the force sensing integrated microgripper. Because most of the displacement is caused by the rotation at the end of the elastic element, we simplify the cantilever structure as a mass spring system ignoring the rotation of the cantilever (Figure 4-9).

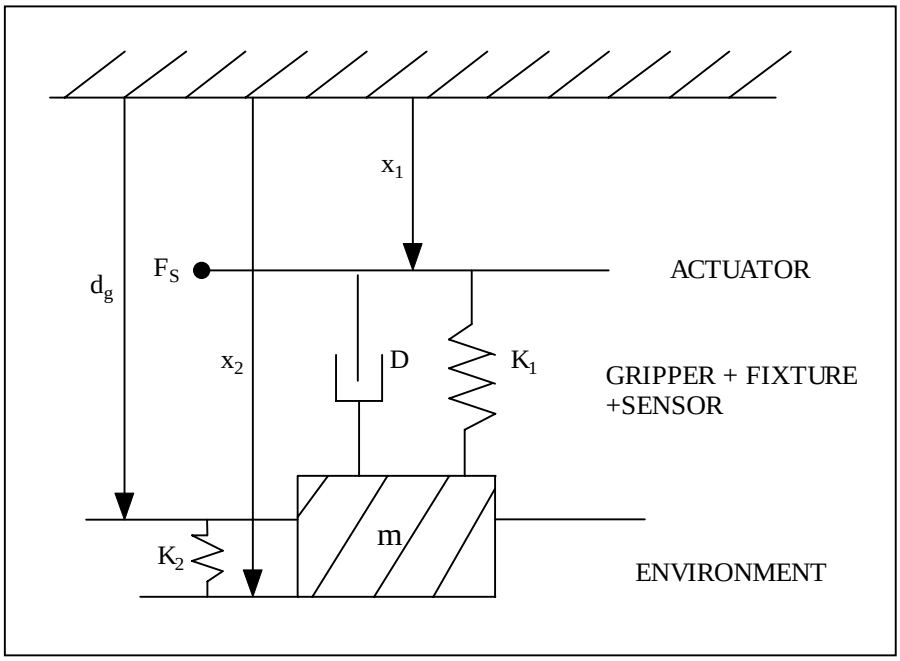

Figure 4-9 Simulated model of end-effector and environment.

The whole system was described by the following equations:

$$F_s = -K_1(x_2 - x_1) - D(\dot{x}_2 - \dot{x}_1) \tag{4.1}$$

where F_s is the output of the force sensor and K_1 and D are stiffness and damping ratio of the elastic element. D is added to make the system stable and K_1 was calculated by:

$$K_1 = \frac{f_p}{\delta} \tag{4.2}$$

f_p and δ have been defined before.

$$m\ddot{x}_2 = K_1(x_2 - x_1) + D(x_2 - x_1) + K_2 r(x_2 - d_g) \tag{4.3}$$

where d_g decides the gap between the part and scaffold before assembly, m is the mass of the tungsten tip and its fixture and:

$$r = \begin{cases} 0 & x_2 < d_g \\ 1 & x_2 \geq d_g \end{cases} \tag{4.4}$$

which means that before contact there is no environment force.

Thereby the system equation can be rewritten as:

$$F_s = K_2(x_2 - d_g) - m\ddot{x}_2 = -K_1(x_2 - x_1) - D(\dot{x}_2 - \dot{x}_1) \tag{4.5}$$

Figure 4-10 shows the system control loops. The inner loop is a precise position control loop, realize by the commercial stage itself. The outer loop is admittance force control loop.

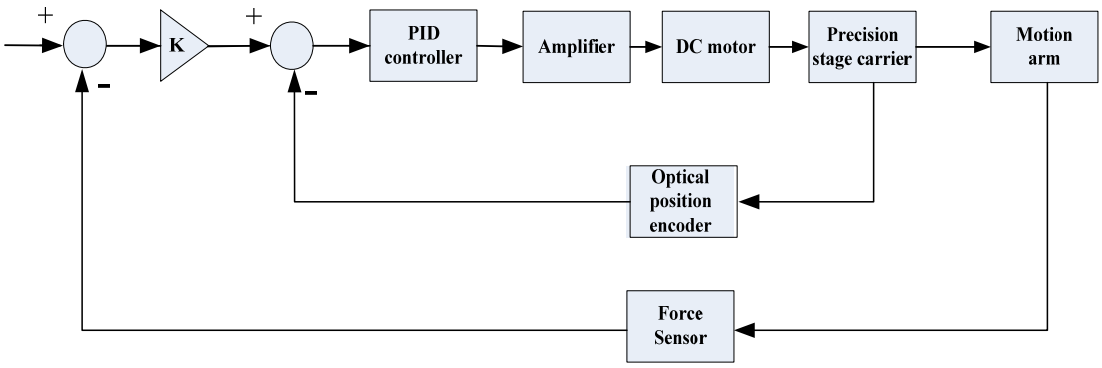

Figure 4-10 System control loop.

As analyzed in previous sections, the objective of the real-time force control is to achieve a smooth force profile during the last steps of the insertion process, so as to protect the micro parts from being damaged by excessive forcee, and at the same time realize a fast assembly. To follow the desired trajectory, a force-based admittance control was proposed and implemented. In mechanical systems, an admittance is a dynamic mapping from force

to motion. In other words, an equation (or virtual environment) describing admittance would have inputs of force and would have outputs such as position or velocity. So, an admittance device would sense the input force and "admit" a certain amount of motion. That is exactly what we need to do in the force control of the commercial actuator: sensing the force, then using it as a reference for the next position the stage should go, hence controlling the force.

The objective of the force control is to realize a fast and safe assembly process, and so the ideal force profile of the actuator is to move very fast when there is no interaction force between the gripper and the environment, and slow down when there is force detected. The velocity should decrease constantly according to the increase of the force, and the last steps should be very slow before it stops without any overshoot, which may cause damage to the parts and the gripper. And to fulfill these requirements, the following admittance law was implemented:

$$\Delta X = k \cdot \Delta F \tag{4-6}$$

where ΔX is the distance the stage should go for next step, ΔF is the difference between the desired force and the measured force from the sensor, k needs to be tuned to derive the desired force profile which contains shortest stable time and minimum overshoot.

The suitable dynamics was derived from simulations and experiments of the real assembly task. MATLAB Simulink was used to do the numerical simulations.

Different values of k was implemented, and results are shown in Figure 4-11. From the results, it can be seen that with increasing the gain k, the assembly time decreases, and when k reaches 40, the assembly time is less than 0.5sec, and there is no obvious overshoot. When k exceeds 40, the assembly time didn't decrease remarkably, and overshoot can be observed.

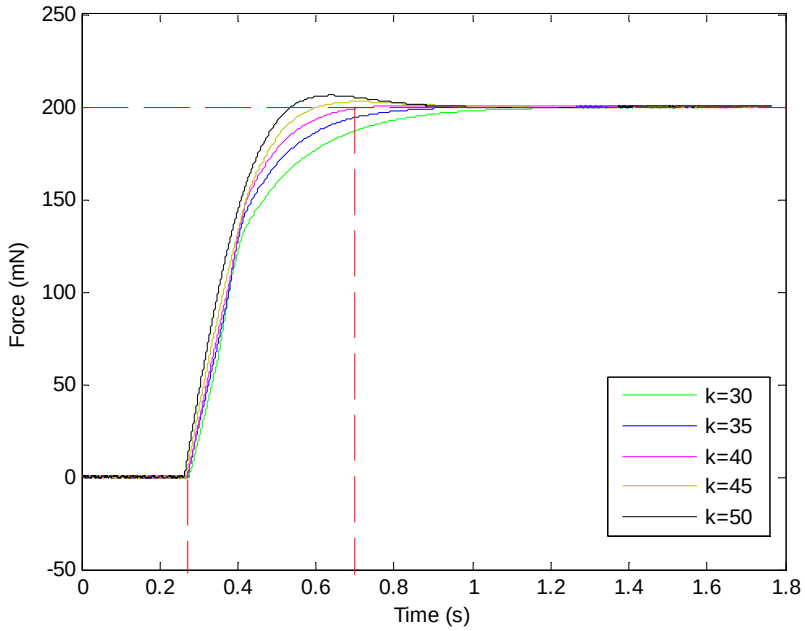

Figure 4-11 Effect of k to the insertion process.

Finally $k = 40$ was selected. The simulation result shows a good tracking of the desired force trajectory: (a). Fast insertion: the insertion can be completed in about one second, which is ideal for the task; (b). Smooth insertion: there is no vibration of force during the last steps of the insertion, which may cause unstable of the system; (c). No obvious overshoot: the gripper can stop at the desired force without overshoot as observed in open-loop control, thus protect both the gripper and the part from impact damage.

Then a series of experiments were done to evaluate the efficiency of the admittance controller by implementing it to the desktop workstation. The stage was set a maximum velocity of $16mm/s$ and the acceleration at $150mm/s^2$, which is recommended by the manufacturer of the stages to ensure the best performance. Sampling time was set to $5m\sec$.

Different conditions are tested for the grasping process, which includes accurate insertion with almost no position error between the axes of the gripper tip and the hole in the part, moderate position error of about $25\mu m$, large position error of about $50\mu m$ and position error larger than $50\mu m$, and the insertion results are shown in Figure 4-10. During the process, the gripper goes down, inserts into the hole, and the friction between the surfaces increases along with the insertion. When the gripper tip is fully inserted, the pushing shoulder touches the upper surface of the part, and the insertion action continues until the force reaches $200mN$ to ensure a fully grasping of the part, and then the gripper lifts with the part attached to it.

When there is almost no position error, the force increases continuously and smoothly, and the insertion time is about $0.5\sec$ (Figure 4-12A).

When there is position error, the force increases roughly first, and then it drops after reaching some value, and then increases again, and this time smoothly (Figure 4-12B, C). This may because when the gripper tip first touches the hole, there is static friction between the surfaces, and when it exceeds a threshold, it turns to be dynamic friction just

like insertion with no position error. Along with the increasing of the position error, the insertion increases, but the force is still controlled as desired.

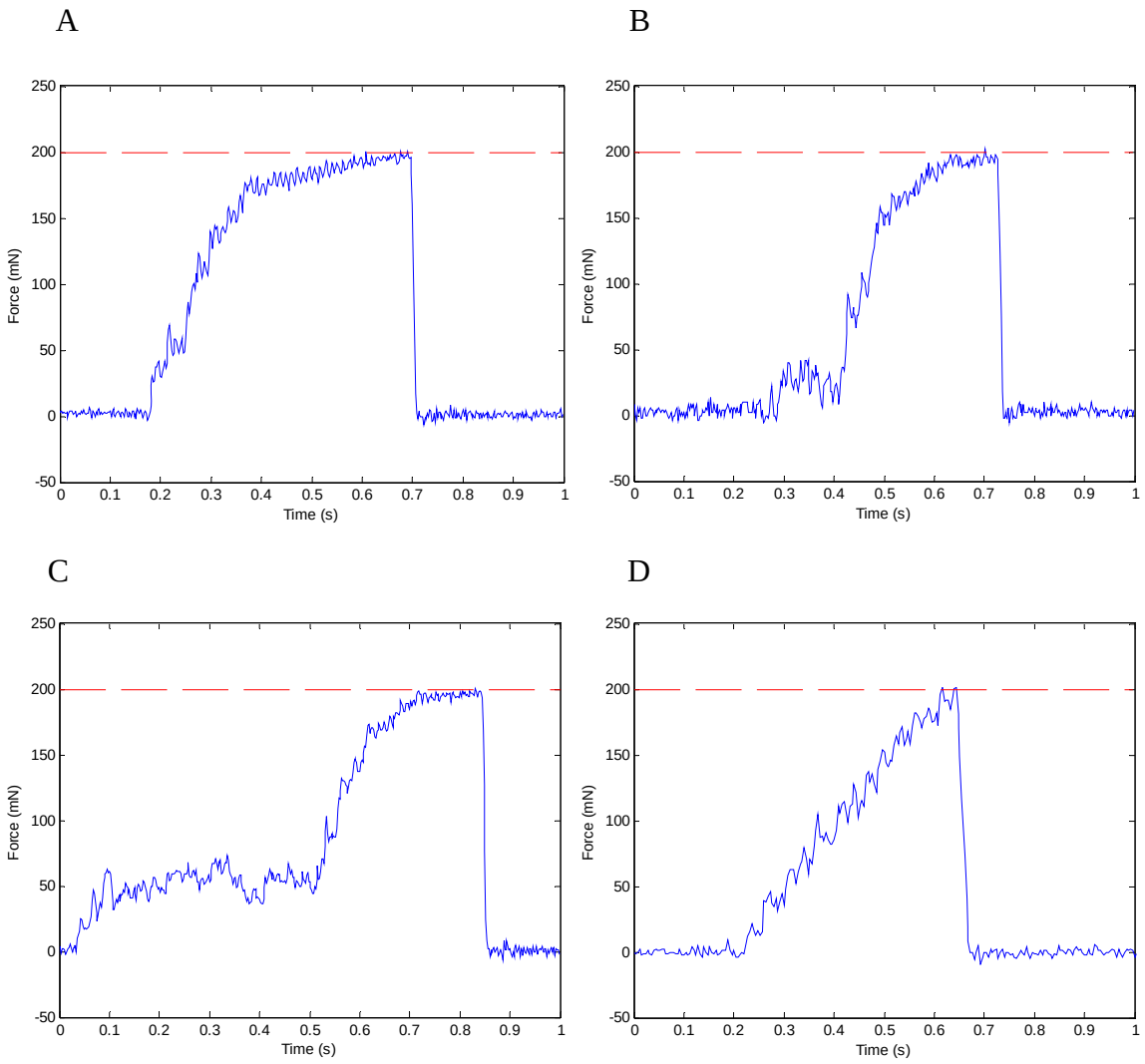

Figure 4-12 Experimental result of admittance controller for grasping process with different tip and hole position errors: (A) No position error; (B) Moderate position error (about $25\mu m$); (C) Large position error (about $50\mu m$); (D) Position error larger than $50\mu m$, cannot insert.

When the position error exceeds $50\mu m$, which means that the axes of the gripper tip is outside the hole, the gripper tip will hit the upper surface of the part. The force increases linearly, but can still stop at the limit without damaging anything.

Then the controller was tested for assembly process. Because the current fabrication process of parts cannot realize a slope shape of the notch with a wider opening, so position error between the two layers during the assembly will not be as large as that during the grasping period. When the position error is smaller than $5\mu m$, the part can be easily assembled in about $0.7\,\text{sec}$, and controller works well (Figure 4-13A, B).

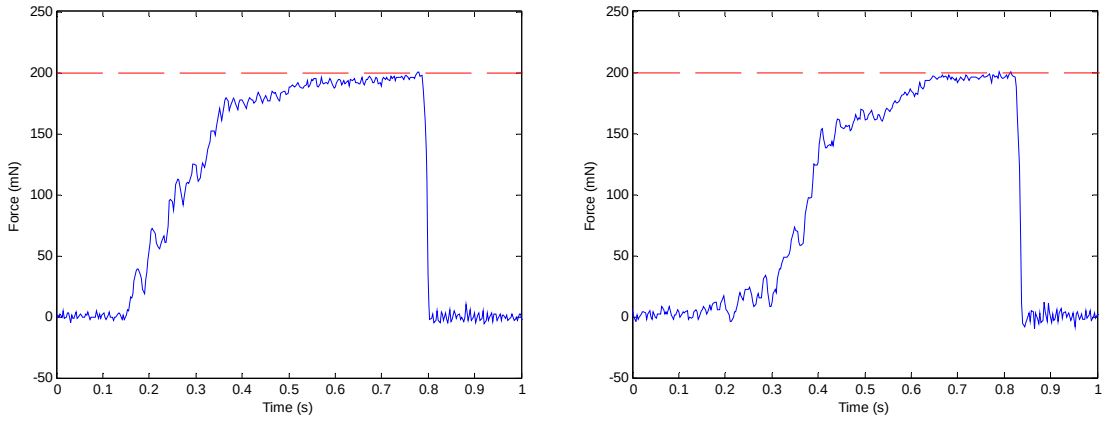

Figure 4-13 Experimental result of admittance controller for assembly process with no position error (A) and $5\mu m$ position error (B).

4.4 ASSEMBLY EXPERIMENTS AND RESULTS

4.4.1 MICRO PART FABRICATION

In our project, 3D Lego®-like micro parts were chosen to build scaffolds of various shapes, which are held together by the friction forces between the micro parts. As mentioned in previous sections, the new micro parts were modified based on those previously used. The design of the micro parts allows the part to be assembled from one after another from above using only the dedicated computer-controlled 5-DOF workstation. The architecture of the scaffold is such that all parts are connected after a minimal number of layers and are homogeneously constrained within the scaffold. The formed pores on the scaffold have a dimension of about 30~40 microns suitable to accommodate bone cells. The design of the micro part can be seen in figure 4-14.

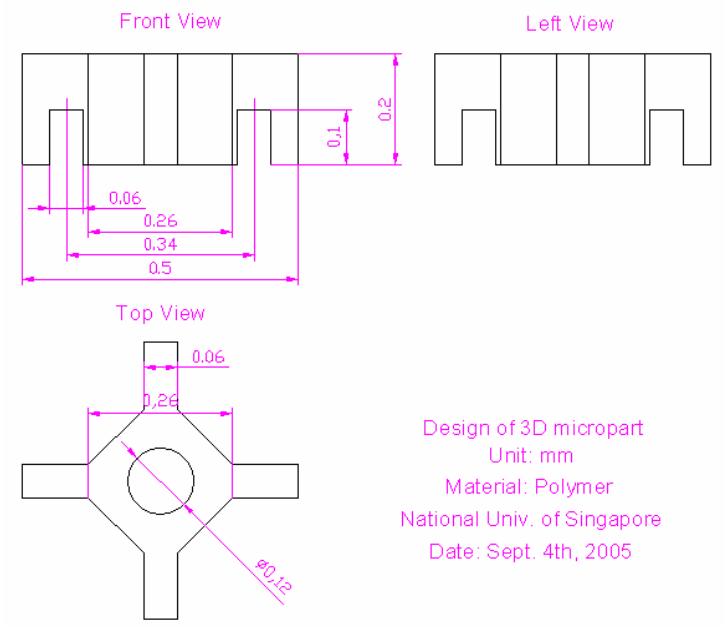

Figure 4-14 Building block CAD drawing.

The hole at the centre of the part is designed particularly to interface the micro probe gripper. With the new gripper, it is easy to pick up and orientate the part. To facilitate assembly, the material should be sufficiently compliant to allow deformation and thus be error tolerant. This facilitates the assembly by force-fitting which also helps to hold parts together tightly after assembly.

Although the ultimate material will be bioabsorbable and biodegradable, now we use SU-8 to fabricate part for experiment. The fabrication of these micro parts is challenging due to their small size ($0.5\times0.5\times0.2mm$ overall, $0.06mm$ thickness) and complex 3-D shape. To facilitate the microassembly process, another challenge is the requirement that the parts need to be stably fixed on the wafer but at the same time easily removed by the gripper. The former requirement is needed to facilitate final fully automated assembly because the position and orientation of each micro part relative to the wafer will be known.

The fabrication process has been described in detail in (Zhang et al, 2003). The fabrication process can be divided into two main steps. First plateaus were created on the silicon wafer, which are used to form the notches of the micro parts in a subsequent step. Then a $0.2mm$ thick layer of SU-8 100 is applied on the wafer and photo-patterned to create the "cross" shapes. The detailed steps are described in Figure 4-15 and Figure 4-16.

The whole process has the following features:

1. SU-8 is used as the material for the parts because it is biocompatible, photo-patternable and can form a thick layer of $200\mu m$ with a single spinning step;

2. The 3-D profile is obtained by combining molding on a patterned Si substrate and photolithography. The extremely flat surface of the SU-8 layer during the fabrication process is achieved by careful control of the reflow of the SU-8;
3. A large number of micro parts can be fabricated at the same time and are positioned in a regular matrix fashion to facilitate grasping by the gripper in a subsequent automated assembly process;
4. A sacrificial layer of thermally grown silicon dioxide is placed between the polymer micro parts and the substrate. Etching of this sacrificial layer is stopped before its complete dissolution so that each micro part remains attached to the base wafer held onto the latter by only a small piece of material. This allows the parts to be easily detached from the base wafer subsequently.

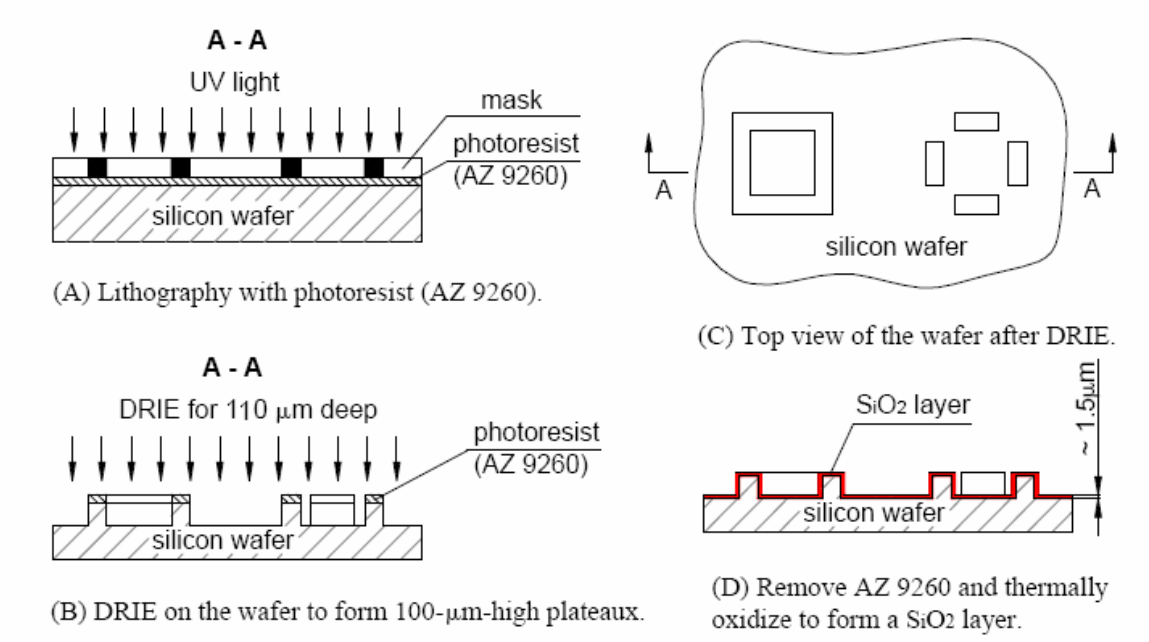

Figure 4-15 Lower layer fabrication process of part.

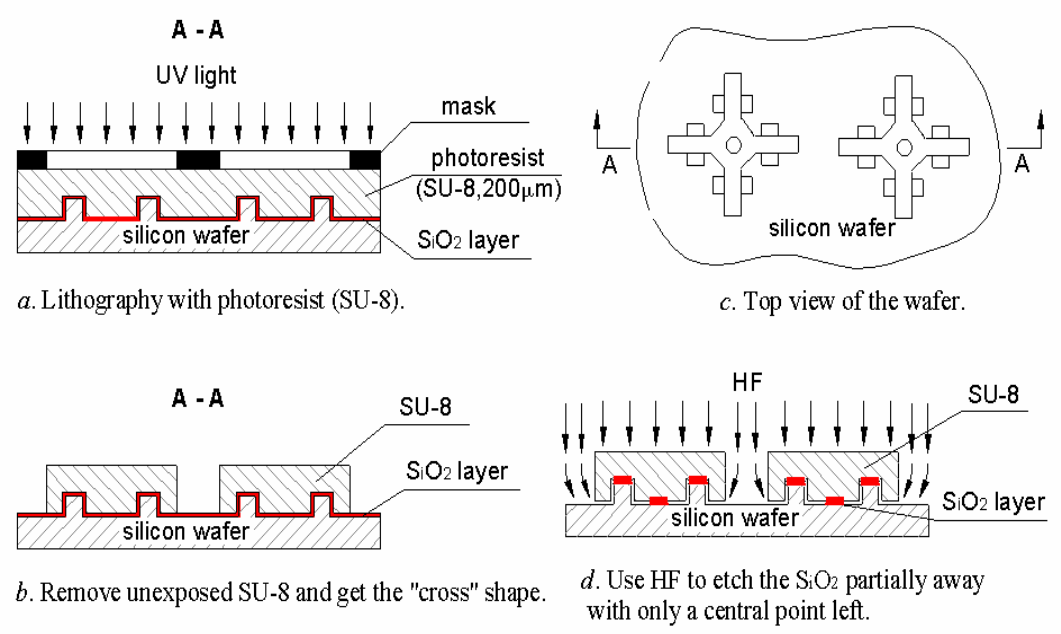

Figure 4-16 Upper layer fabrication process of part.

4.4.2 ASSEMBLY PROCESS AND RESULTS

The whole assembly process is shown in Figure 4-17.

1. Manual calibration**:**

   Assembly process begins with manual calibration. Manual calibration will be done in a teleoperation fashion. First, move the mark on scaffold wafer into the field of view of the microscope, and save a picture to generate a template. Set all the position encoders to zero, and define the position as “home”, which is the assembly position of the first part. Second, move the part magazine under the microscope and locate the first part with the help of two side-view microscopes. The accuracy can be less than 5 micron based on past experiences. Save the position encoder value, i.e., the x and y coordinate of the part. Thereby the relative position of the first part to its assembly

position is derived. Third, pick up the part and give a “go home” command, the stages will move until the part is right above its assembly position. Insert the part into its assembly position. If the part can be assembled smoothly, the manual calculation is valid. Otherwise, repeat the process until the part can be smoothly assembled.

2. Calculate the next part’s position**.**

   Parts align on the wafer regularly after fabrication, and the relative position of every two parts is fixed. Thereby the next part’s position can be calculated.

3. Go to next part.

   Move the gripper to the part. It should be just over the hole of the part.

4. Pick up a part.

   This is the only action of moving down the gripper and lifting the part. The process is controlled by the admittance controller. Failure in picking up of the part it will be discussed in following steps.

5. Calculate the next inserting position.

   The relative assembly position of every two part on the wafer are strictly uniform, thereby its coordinates can be calculated.

6. Go to the inserting position.

   Send a command to stages to move the part to the assembly position on the scaffold wafer.

7. Assemble part.

   Try to assembly part into scaffold. This process is controlled by the admittance controller.

8. Self calibration.

After the assembly of a certain number of parts, the accumulated error may reach 10 microns, which will cause misalignment of the next part. Send a “go home” command to the stage. Take picture of the current view. Compare it with the template picture and calculate the position error of the mark. Move the stages until the error is eliminated.

9. Decision 1.

   From information of self-calibration and scaffold status, it can be decided whether the current part has been tried to assemble twice.

10. Abandon.

    Send a command to x-y stage, move the part to the disposal area and abandon the part.

11. Decision 2.

    From the information of part magazine status and abandon counter to decide how many times parts have been abandoned consecutively. If abandon action has been called 3 time in a row, that means the system needs re-calibration.

12. Error alarm.

    Error alarm and stop the whole system.

13. Decision 3.

    From scaffold status data, check if the scaffold is completed. If the scaffold is completed, then go to ‘over’. If the scaffold is not completed and N parts have been assembled without self-calibration, then go to self-calibration.

14. Over.

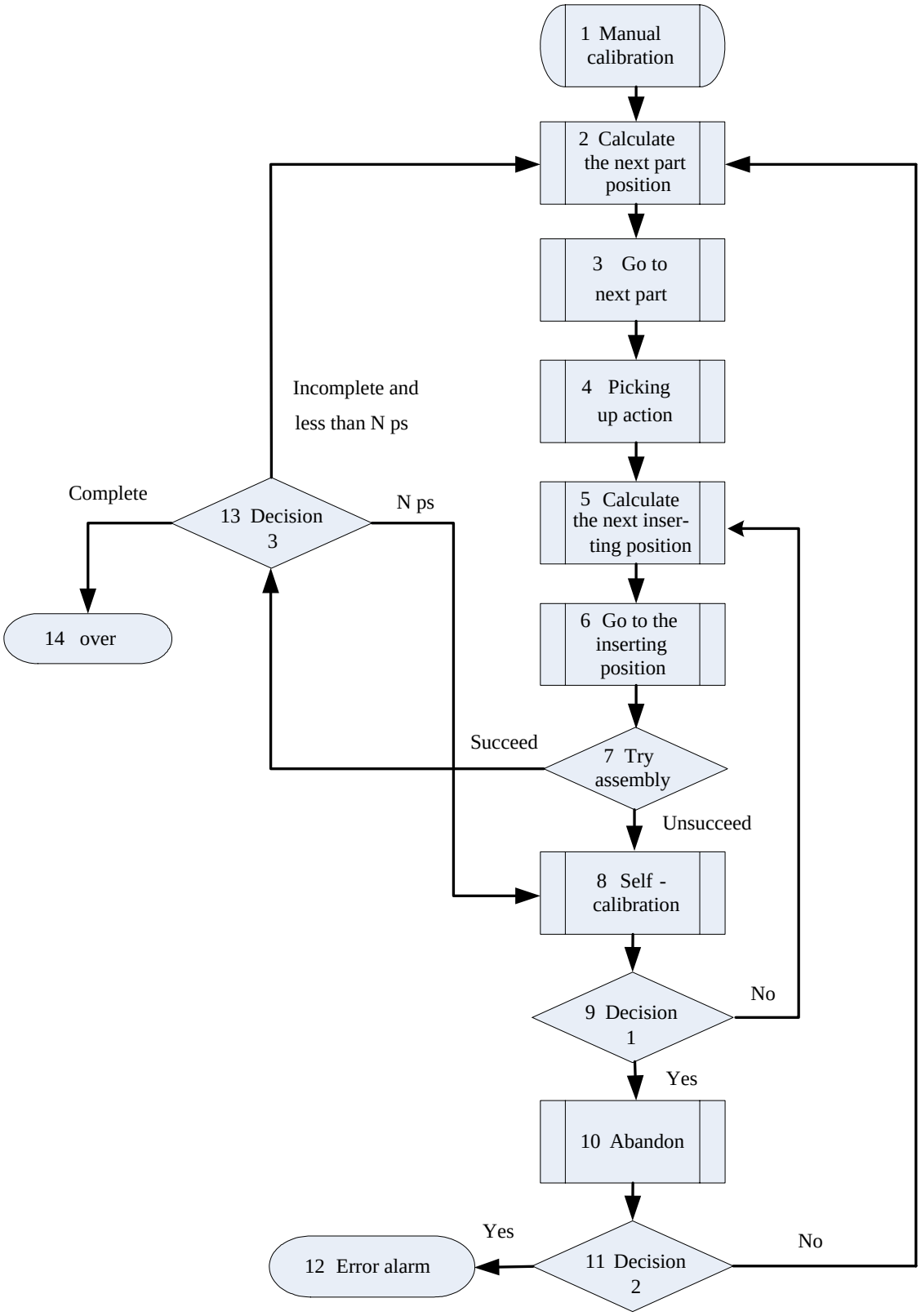

Figure 4-17 Flow chart of assembly process.

A three-layer scaffold was built as shown as shown in Figure 4-18.

After assembly, the sticking force between parts has also been tested. Glue was put on the gripper tip, so that after it is inserted into the part, the part will be stuck to it. Then the part was pushed to the lower layer until the force reached the desired value, and then it was pulled out by lifting the gripper. The force of the whole process was recorded (Figure 4-19). Negative force of about $40mN$ was detected, which is twice more than the analysis value, which is only $15mN$ (Zhang, 2005).

Error analysis shows that the position error in x-y plane decreases along with the increasing of the number of layers (Zhang et al, 2002), and the same result is derived from the experiment through measuring the distance between the adjacent two parts. And with increasing layers, the assembly process becomes easier. The reason for this phenomenon might be because the lower structure becomes more flexible compared to the stiff zero-plate.

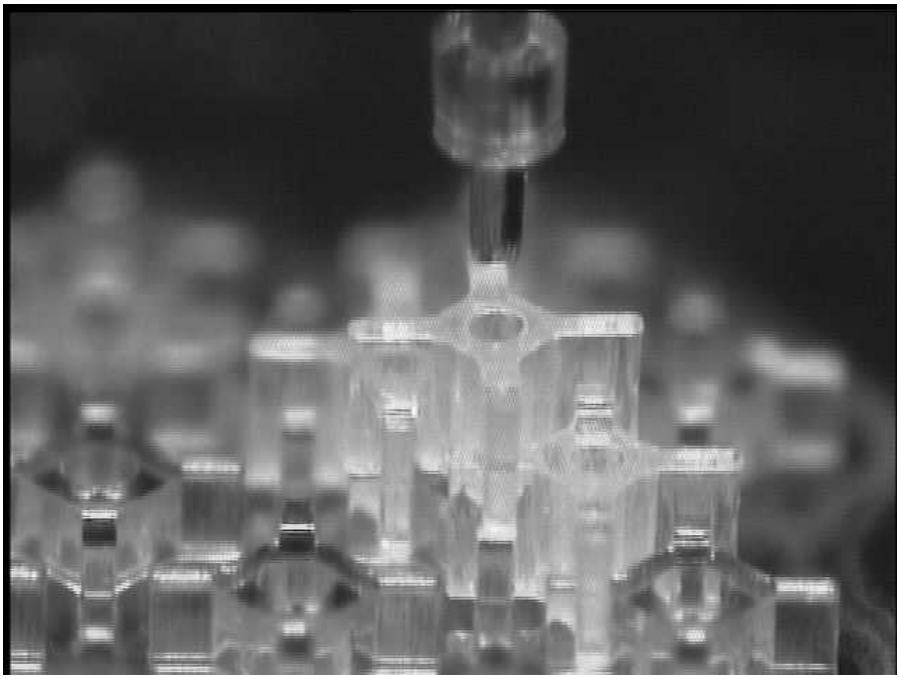

Figure 4-18 A three-layer scaffold.

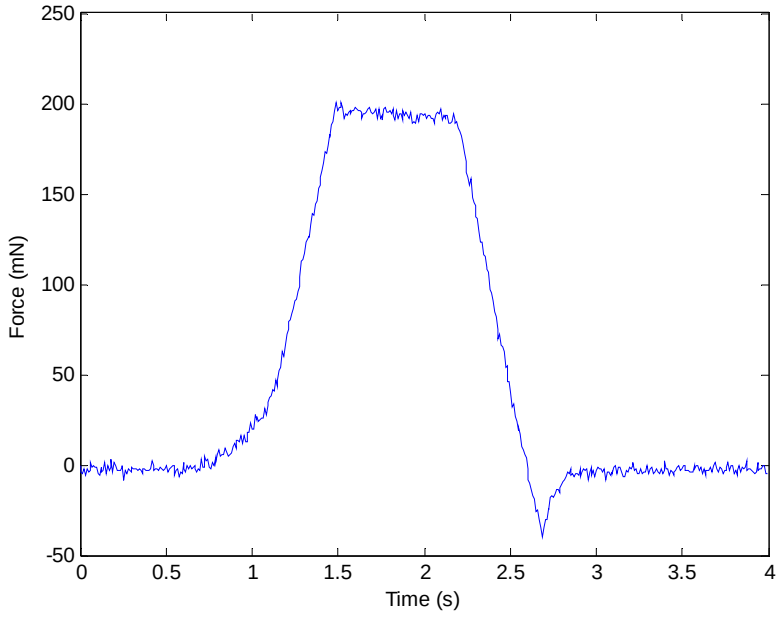

Figure 4-19 Sticking force between parts after assembly.

4.5 CONCLUSION

This chapter presented both the software and hardware of the dedicated precision workstation, and the force-controlled automatic assembly of scaffold for tissue engineer has been carried out successfully.

The dedicated desktop workstation has five DOF, which was realized by one translation stage in x direction, one translation stage in y direction, one translation stage and one vertical stage in z direction, and one rotation stage in z direction. An electro-chemical etched micro probe gripper with a polymer pushing shoulder was fixed to the z stage for grasping and assembling. The grasping was achieved by the friction between the probe gripper tip and the hole in the part, and the assembly was achieved by the force generated by the pushing shoulder, and the forces can be controlled through controlling the dimension of the gripper and the part. A microscope was fixed above the workspace to snap the top view which was used to guide the locating of the part. During the initialization, two more microscopes were needed, and after that, all the vision feedback is from the top view microscope.

A force-based admittance controller was proposed and implemented to the assembly process, which was used to control the grasping as well as the assembling action, i.e., the movement in z direction. The controller is robust to the environment, for it can assure a successful assembly despite the variance of the part dimension, and protect the part and the gripper from any damage even when the allocating of the part was not so accurate. And using the controller the efficiency can be increased dramatically.

During the assembly, side slide of the part on the wafer was observed when the gripper was inserted into the hole as well as assembling the part into the lower layer. Through modify the design of the mechanical structure, the slide can be minimized and has no influence to the process. After assembly, the parts stick together tightly, and position error exists in layers of assembled scaffold, but the amount will decrease with increasing layers.

Chapter 5

Conclusions and future work

5.1 CONCLUSIONS

Automatic microassembly poses new challenges and problems in design and control of hardware and software, and the main problem of current approaches is the lack of realtime control of the assembly force or insertion force, to achieve a high efficiency and high yield assembly process. Previously the process was usually controlled through image processing, but it is slow, costly, difficult to program, and susceptible to reflection and other noise.

To achieve a fast and high yield 3D microassembly process, an automatic z-axis microassembly strategy was proposed, implemented, and evaluated in some tissue engineering scaffold assembly experiments. The two main contributions of this thesis are the development of a novel force sensor integrated probe gripper and an admittance force controller.

The objective of this project is to realize a fully automatic assembly of the 3D scaffold for tissue engineering, and the strategy is to use the combination of vision feedback and force feedback. To fulfill this purpose, a computer controlled five DOF dedicated desktop workstation was built based on the previous 4 DOF workstation. Two translation stages

are fixed in x and y direction to accomplish the transfer of parts from the original wafer to the target wafer. One vertical stage is fixed on the x stage to work as the assembly platform and keep the top layer of the scaffold in the focusing plane of the microscope. One translation stage is fixed in z direction to achieve the movement of the endeffector in z direction. One rotation stage was fixed on the z stage for initializing the angle of the gripper.

A force sensing integrated micro gripper was designed and fabricated to accomplish the grasping and assembling actions. The micro probe gripper was made of some commercially available tungsten rod using electro-chemical etching technique. Tungsten was chosen as the material to achieve high stiffness and small dimension (100 μm in diameter). The force sensor was made by attaching two semiconductor strain gauges on a home-made sensor body, and the finished sensor has the range of several Newton and milli-Newton resolution. The filtered force signal from the sensor has good linearity and low noise.

A force-based admittance control was proposed and implemented to the system using the force feedback from the sensor to control the grasping and assembling process. Experiments show that during open-loop control of the grasping and assembling process, the force changes rapidly, and there is excessive overshoot observed which may cause damaging of the fragile micro parts and the micro gripper. By implementing the admittance controller, the force during both the grasping and the assembling process increases smoothly, and the gripper can stop at the desired position sharply. The controller

can ensure a fast assembly process and robust to any variance in the micro parts dimension, which is very important for the dimension is impossible to be controlled precisely during fabrication.

The micro part is redesigned to meet the requirements of the automatic assembly and fabricated using photolithography technique. With the new structure, the parts can be built to any specific shape for different purpose.

Assembly experiments were carried out to evaluate the system. During the initialization, two extra microscopes are used for calculating the position through side view. Another microscope is fixed above the assembly workspace to snap the top view which is used to locate the grasping and assembling position and thus to guide the movement in the x-y plane. And then the movement in z direction is achieved through the admittance controller.

Multi-layer scaffold has been built using the developed system. And we note that apart from the assembly tasks, this automated workstation can be used e.g. for manipulating biological cells or testing silicon chips.

5.2 FUTURE WORK

This thesis's emphasis was laid on evaluating the feasibility of achieving the automatic assembly using top view and a force control, and currently the system is work in a semi-automatic way. To realize the fully automatic assembly, and finally put the system into practice usage, some modification and improvement should be done.

The first is to implement machine vision into the system to replace the current method of locating the grasping and assembling position manually. Currently it takes several seconds to assemble one part, and most of the time is consumed on the location part. The accuracy using manual location is not high, which may cause extra friction during the insertion and even misalignment of the gripper tip and the hole. Therefore, it is essential to implement the locating using machine vision. There will be position error after the part was assembled on the lower layer, and after each part is assembled, the position error may vary a bit, so the best way to implement the machine vision is to take a photo of the lower layer, and then compare the figure with some preloaded standard figure using some pattern matching technique to calculate the position for the next movement. The micro part is made from some transparent material, which makes it difficult to be discriminated through the microscope. A solution could be to dye the part.

Second, currently the system is just for evaluating the proposed scaffold assembly technique. For practical usage, the following issues need to be addressed.

- Now the material of the micro part is SU-8, but later the material should be biocompatible and bioabsorbable.
- The fabrication technique should be improved or replaced with some more precise and simple method. The current way has several steps, and thus the quality of the part may be affected by a lot of factors, and the photolithography process may damage the biomaterial. Micromolding technique could be a practical alternative, for it has no

special requirements of the material, the process is simple, and by carefully arranging multiple molds, the current assembly process can be used.

- In practical use, the part will first be coated with cells, and this process must be accomplished in liquid to keep the cell alive, as well as the assembly process. Then the gripper should be made from some biocompatible material or coated with some biocompatible material. Implementation of the machine vision under liquid should also be considered.

Bibliography

[1] **Arai F., Kawaji A., Sugiyama T., Onomura Y., Ogawa M., Fukuda T., Iwata H., Itoigawa K.,** 3D micromanipulation system under microscope, IEEE International Symposium on Micromechatronics and Human Science, Nov. 25-28, pp. 127-134, 1998.

[2] **Arai F., Motoo K., Fukuda T., Katsuragi T.,** High sensitive micro touch sensor with piezoelectric thin film for micro pipetting work under microscope, IEEE International Conference on Robotics and Automation, Apr. 26-May 1, vol. 2, pp. 1352-1357, 2004.

[3] **Arai F., Nonoda Y., Fukuda T., Oota T.,** New force measurement and micro grasping method using laser raman spectrophotometer, IEEE International Conference on Robotics and Automation, Apr. 22 - 28, vol. 3, pp. 2220 - 2225, 1996.

[4] **Berkelman P.J., Whitcomb L.L., Taylor R.H., Jensen P.,** A miniature microsurgical instrument tip force sensor for enhanced force feedback during robot-assisted manipulation, IEEE Transactions on Robotics and Automation, Oct., vol. 19, Issue 5, 2003.

[5] **Böhringer K. F., Fearing R. S., Goldberg K. Y.**, Chapter Microassembly, The Handbook of Industrial Robotics (2nd edition), pp. 1045-1066, John Wiley & Sons, February 1999.

[6] **Brussel H.V., Peirs J., Revnaerts D., Delchambre A., Reinhart G., Roth N., Weck M., Zussman E.,** Assembly of Microsystems, Annals of the CIRP, pp.451-472, vol.49(2), 2000.

[7] **Bruzzone L.E., Molfino R.M., Zoppi M.,** Modelling and control of peg-in-hole assembly performed by a translational robot, IASTED International Conference on Modelling, Identification and Control, Feb. 18-21, pp. 512-517, 2002.

[8] **Carrozza M.C., Eisinberg A., Menciassi A., Campolo D., Micera S., Dario P.,** Towards a force-controlled microgripper for assembling biomedical microdevices, J. Micromech. Microeng., pp.271-276, vol.10, 2000.

[9] **Chao Y.C., Lee Y.J., Liu John, Shen G.S., Tsai F.J.,** Development of probing mark analysis model, IEEE International Conference on Electronic Packaging Technology, Oct. 28-30, pp. 40-43, 2003.

[10] **Clanton S.T., Wang D.C., Chib V.S., Matsuoka Y., Stetten G.D.,** Optical merger of direct vision with virtual images for scaled teleoperation, IEEE Transaction on Visualization and Computer Graphics, vol.12, issue 2, 2006.

[11] **Cohn M.B., Böhringer K.F., Noworolski J.M., Singh A., Keller C.G., Goldberg K.Y., Howe R.T.,** Microassembly technologies for MEMS, Proc. SPIE Micromachining and Microfabrication, pp.2-16, 1998.

[12] **Craig J.J.,** Introduction to robotics: mechanics and control, 2nd ed., Reading, Mass.: Addison-Wesley, 1989.

[13] **Dargahi J., Parameswaran M., Payandeh S.,** A micromachined piezoelectric tactile sensor for an endoscopic grasper-theory, fabrication and experiments, IEEE Journal of Microelectromechanical Systems, vol. 9, Issue 3, 2000.

[14] **Deok-Ho Kim, Byungkyu Kim, and Hyunjae Kang**, Force feedback-based microassembly: system integration and experiments, Submitted to IEEE/ASME Transactions on Mechatronics.

[15] **Deok-Ho Kim, Seok Yun, Byungkyu Kim,** Mechanical force response of singling living cells using a microrobotic system, IEEE International Conference on Robotics and Automation, Apr. 26-May 1, vol. 5, pp. 5013-5018, 2004.

[16] **Eisinberg A., Menciassi A., Micera S., Campolo D., Carrozza M.C., Dario P.,** PI force control of a microgripper for assembling biomedical microdevices, IEE Proceedings Circuits Devices Systems, vol.148, Issue 6, pp.348-352, 2001.

[17] **EMSL website:** http://www.emsl.pnl.gov/capabs/instruments/instrument_pages/1037.shtml.

[18] **Enikov E.T., Minkov L.L., Clark S.,** Microassembly experiments with transparent electrostatic gripper under optical and vision-based control, IEEE Transactions on Industrial Electronics, August, pp.1005-1012, vol.4, 2005.

[19] **Enikov E.T., Nelson B.J.,** Three-dimensional microfabrication for a multi-degree-of-freedom capacitive force sensor using fibre-chip coupling, Journal of Micromechanics and Microengineering, vol. 10, Issue 4, pp. 492-497, 2000.

[20] **Fahlbusch S., Fatikow S.,** force sensing in microrobotic systems-an overview, IEEE International Conference on Electronics, Circuits and Systems, Sept. 7-10, pp.259-262, vol.3, 1998.

[21] **Fatikow S., Rembold U.,** An automated microrobot-based desktop station for micro assembly and handling of micro-objects, IEEE Conference on Emerging Technologies and Factory Automation, Nov. 18-21, pp.586-592, vol.2, 1996.

[22] **Fatikow, S., Seyfried, J., Fahlbusch, St., Buerkle, A. and Schmoeckel, F.,** A flexible microrobot-based microassembly station, IEEE International Conference on Emerging Technologies and Factory Automation, Oct. 18-21, pp.397-406, vol.1, 1999.

[23] **Fearing R.S.,** Survey of sticking effects for micro parts handling, IEEE/RSJ International Conference on Intelligent Robots and Systems, pp. 212-217, vol. 2, 1995.

[24] **Fischer R., Zuhlke D., Hankes J.,** Gripping technology for automated micro-assembly, Proc. SPIE Microrobotics and Microsystem Fabrication, Oct. 16-17, pp. 12–19, vol. 3202, 1998.

[25] **Fung C.K.M., Li W.J., Elhajj, I., Ning Xi,** Internet-based Remote Sensing and Manipulation in Micro environment, IEEE/ASME International Conference on Advanced Intelligent Mechatronics, July 8-12, pp.695-700, vol.2, 2001.

[26] **Ge Yang, Gains J.A., Nelson B.J.,** A flexible experimental workcell for efficient and reliable wafer-level 3D microassembly, IEEE International Conference on Robotics and Automation, May 21-26, pp.133-138, 2001.

[27] **Ge Yang, Gains J.A., Nelson B.J.,** A supervisory wafer-level 3D microassembly system for hybrid MEMS fabrication, Journal of Intelligent and Robotic Systems, 37: 43-68, 2003.

[28] **Grutzeck H., Kiesewetter L.**, Downscaling of grippers for micro assembly, Microsystem Technologies, 8:27–31, 2002.

[29] **Haliyo D.S., Regnier S.,** Advanced applications using [mu]MAD, the adhesion based dynamic micro-manipulator, IEEE/ASME International Conference on Advanced Intelligent Mechatronics, July 20-24, pp.880-885, vol.2, 2003.

[30] **Haliyo D.S., Rollot Y., Regnier S.,** Manipulation of micro-objects using adhesion forces and dynamical effects, IEEE International Conference on Robotics and Automation, May 11-15, pp.1949-1954, vol.2, 2002.

[31] **Hara H., Yokogawa R., Kai Y.,** Evaluation of task performance of a manipulator for a peg-in-hole task, IEEE International Conference on Robotics and Automation, pp. 600-605, 1997.

[32] **Healy K.E., Tsai D., Kim J.E.,** Osteogenic cell attachment to biodegradable polymers, Mater Res Soc Symp Proc, 252:109, 1992.

[33] **Ikuta K., Nokata M., Aritomi S.,** Biomedical micro robots driven by miniature cybernetic actuator, IEEE Workshop on Micro Electro Mechanical Systems, pp.263-268, Jan 25-28, 1994.

[34] **Jungyul Park, Sangmin Kim, Deok-Ho Kim, Byungkyu Kim, Sangjoo Kwon, Jong-Oh Park, Kyo-Il Lee,** Advanced controller design and implementation of a sensorized microgripper for micromanipulation, IEEE International Conference on Robotics and Automation, Apr. 26-May 1, vol. 5, pp. 5025-5032, 2004.

[35] **Kaneko K., Tokashiki H., Tanie K., Komoriya K.,** A development of experimental system for macro-micro teleoperation, IEEE International Workshop on Robot and Human Communication, pp. 30-35, July 5-7, 1995.

[36] **Kaneko K., Tokashiki H., Tanie K., Komoriya K.,** Impedance shaping based on force feedback bilateral control in macro-micro teleoperation system, IEEE

International Conference on Robotics and Automation, pp.710-717, vol.1, Apr. 20-25, 1997.

[37] **Keller C.G., Howe R.T.,** Hexsil tweezers for teleoperated microassembly, IEEE Annual International Workshop on Micro Electro Mechanical Systems, Jan. 26-30, pp.72-77, 1997.

[38] **Kim S.S., Utsunomiya H., Koski J.A., Wu B.M., Cima M.J., Sohn J., Mukai K., Griffith L.G., Vacanti J.P., Vacanti J.P.,** Survival and function of hepatocytes on a novel three-dimensional synthetic biodegradable polymer scaffold with an intrinsic network of channels, Ann Surg, 228(1):8-13, 1998.

[39] **Kobayashi H., Nakamura H., Tatsuno J., Iijima S.,** Micro-macro tele-manipulation system, IEEE International Workshop on Robot and Human Communication, pp. 165-170, Nov. 3-5, 1993.

[40] **Ku S., Salcudean S.E.,** Design and control of a teleoperated microgripper for microsurgery, IEEE International Conference on Robotics and Automation, Apr. 22-28, vol.1, 1996.

[41] **Lai K.W.C., Chung P.S., Ming Li, Li W.J.,** Automated micro-assembly of surface MEMS mirrors by centrifugal force, IEEE International Conference on Mechatronics and Automation, Aug. 26-31, pp.23-28, 2004.

[42] **Langer R., Vacanti J.P.,** Tissue Engineering, Science, 260: 920-926, 1993.

[43] **Leong K.F., Cheah C.M., Chua C.K.,** Solid freeform fabrication of three-dimensional scaffolds for engineering replacement tissues and organs, Biomaterials, 24:2363–2378, 2003.

[44] **Ljung L.,** System identification – theory for the user, 2nd ed., PTR Prentice Hall, Upper Saddle River, N.J., 1999.

[45] **Ljung L.,** System identification toolbox user's guide, 6th version, MathWorks, 2006.

[46] **Maekawa S., Takemoto M., Kashiba Y., Deguchi Y., Mike K., Nagata T.,** Highly reliable probe card for wafer testing, IEEE Electronic Components and Technology Conference, pp. 1152-1156, 2000.

[47] **McClary K.B., Ugarova T., Grainger D.W.,** Modulating fibroblast adhension, spreading and proliferation using self-assembled monolayer films of alkylthiolates on gold, J. Biomed. Mater. Res., 50(3):429-39, 2000.

[48] **Mikos A.G., Sarakinos G., Lyman M.D., Ingber D.E., Vacanti J.P., Langer R.,** Prevascularization of porous biodegradable polymers, Biotechnol Bioeng., 42:716-23, 1993.

[49] **Mitsuishi M., Tomisaki S., Yoshidome T., Hashizume H., Fujiwara K.,** Tele-micro-surgery system with intelligent user interface, IEEE International Conference on Robotics and Automation, Apr. 24-28, pp.1607-1614, vol.2, 2000.

[50] **Nakagaki H., Kitagaki K., Tsukune H.,** Study of insertion task of a flexible beam into a hole, IEEE International Conference on Robotics and Automation, pp.330-350, 1995.

[51] **Nelson B.J., Yu Zhou, Vikramaditya B.,** Sensor-based microassembly of hybrid MEMS devices, IEEE Control Systems magazine, Dec., pp.35-45, vol.18, issue 6, 1998.

[52] **Nikolai Dechev, William L. Cleghorn, James K.M.,** Microassembly of 3-D microstructures using a compliant, passive microgripper, Journal of microelectronmechanical systems, April, vol.13, No. 2, 2004.

[53] **Park J., Moon W.**, A hybrid-type micro-gripper with an integrated force sensor, Microsystem Technologies, pp.511-519, vol.9, issue 8, 2003.

[54] **Popa D., Byoung H.K., Jeongsik S., Jie Z.,** Reconfigurable microassembly system for photonics applications, IEEE International Conference on Robotics and Automation, pp.1495C500, 2002.

[55] **Quan Zhou, del Corral C., Esteban P.J., Aurelian A., Koivo H.N.,** Environmental influences on microassembly, IEEE/RSJ International Conference on Intelligent Robots and Systems, pp.1760-1765, Oct., 2002.

[56] **Robinson B., Hollinger J.O., Szachowicz E., Brekke J.,** Calvarial bone repair with porous D, L-polylactide, Otolaryng Head Neck, 112(6):707-13, 1995.

[57] **Ruther P., Bacher W., Feit K., Menz W.,** LIGA-microtesting system with integrated strain gauges for force measurement, IEEE Tenth Annual International Workshop on Micro Electro Mechanical Systems, Jan. 26-30, pp.541-545, 1997.

[58] **Seysried J.,** Control and planning system of a micro robot-based micro-assembly station, Proc. of the 30th ISR, Tokyo, Japan, 1999.

[59] **Skidmore G., Ellis M., Geisberger A., Tsui K., Saini R., Huang T., Randall J.,** Parallel assembly of microsystems using Si micro electro mechanical systems, Microelectronic Engineering, June, pp.445-452, vol.67-68, 2003.

[60] **Skidmore G., Ellis M., Geisberger A., Tsui K., Tuck K., Saini R., Udeshi T., Nolan M., Stallcup R., Von Ehr J. II,** Assembly technology across multiple length

scales from the micro-scale to the nano-scale, IEEE International Conference on Micro Electro Mechanical Systems, pp. 588-592, 2004.

[61] **Smith C. S.,** Piezoresistance effect in germanium and silicon," Phys. Rev., pp. 42-49, vol. 94, issue 1, 1954.

[62] **Speich J.E., Goldfarb M.,** An implementation of loop-shaping compensation for multidegree-of-freedom macro-microscaled telemanipulation, IEEE Transactions on Control Systems Technology, vol.3, issue 3, pp.459-464, 2005.

[63] **STM Tips website:** http://www.phys.unt.edu/stm/tips.htm.

[64] **Sulzman A., Breguet J.M., Jacot J.,** Micromotor assembly using high accurate optical vision feedback for microrobot relative 3D displacement in submicron range, IEEE International Conference on Solid-State Sensors and Actuators, June 16-19, pp.279-282, 1997.

[65] **Sun Y., Nelson B.J., Potasek A.S., Enikov E.,** A bulk microfabricated multi-axis capacitive cellular force sensor using transverse comb drives, Journal of Micromechanics and Microengineering, vol. 12, pp. 832-840, 2002.

[66] **Sun Y., Potasek D.P., Piyabongkarn D., Rajamani R., Nelson B.J.,** Actively servoed multi-axis microforce sensors, IEEE International Conference on Robotics and Automation, Sept. 14-19, 294-299, 2003.

[67] **Thompson J.A., Fearing R.S.,** Automating microassembly with ortho-tweezers and force sensing, IEEE/RSJ International Conference on Intelligent Robots and Systems, Oct. 29 – Nov. 3, pp.1327-1334, 2001.

[68] **Tortonese M., Yamada H., Barrett R. C., Quate C. F.,** Atomic force microscopy using a piezoresistive cantilever, Transducers'91, pp. 448-451, 1991.

[69] **Vacanti J.P., Morse M.A., Saltzman W.M., Domb A.J., Peter-Atayde A., Langer R.,** Selective cell transplantation using bioabsorbable artificial polymers as matrices, J Pediatr Surg, 23(1):3-9, 1988.

[70] **Vishay website:** http://www.vishay.com/brands/measurements_group/guide/ib/b129/129index.htm.

[71] **Wang S., Ding J., Yun J., Li Q., Han B.,** A robotic system with force feedback for micro-surgery, Proceedings of the 2005 IEEE International Conference on Robotics and Automation, Apr. 18-22, pp.199-204, 2005.

[72] **Weitz P., Ahlswede E., Weis J., Klitzing K.V., Eberl K.,** A low-temperature scanning force microscope for investigating buried two-dimensional electron systems under quantum Hall conditions, Journal of Applied Surface Science, 157: 349-354, 2000.

[73] **Yannas I.V., Lee E., Orgill D.P., Skrabut E.M., Murphy G.F.,** Synthesis and characterization of a model extracellular matrix that induces partial regeneration of adult mammalian skin, Proc Natl. Acad. Sci. USA, 86:933, 1989.

[74] **Yantao Shen, Ning Xi, Li W.J., Jindong Tan,** A high sensitivity force sensor for microassembly: design and experiments, IEEE/ASME International Conference on Advanced Intelligent Mechatronics, July 20-24, vol. 2, pp. 703-708, 2003.

[75] **Yantao Shen, Ning Xi, Li W.J., Yongxiong Wang,** Dynamic performance enhancement of PVDF force sensor for micromanipulation, IEEE/RSJ International Conference on Intelligent Robots and Systems, Aug. 2-6, pp. 2827-2832, 2005.

[76] **Yantao Shen, Ning Xi, Pomeroy C.A., Wejinya U.C., Li W.J.,** An active micro-force sensing system with piezoelectric servomechanism, IEEE/RSJ International Conference on Intelligent Robots and Systems, Aug. 2-6, pp. 2381-2386, 2005.

[77] **Yantao Shen, Ning Xi, Wejinya U.C., Li W.J.,** High sensitivity 2-D force sensor for assembly of surface MEMS devices, IEEE/RSJ International Conference on Intelligent Robots and Systems, Sept. 28-Oct. 2, vol. 4, pp. 3363-3368, 2004.

[78] **Young-bong Bang, Kyung-min Lee, Kook J., Wonseok Lee, In-su Kim,** Micro parts assembly system with micro gripper and RCC unit, IEEE Transactions on Robotics, June, pp.465-470, vol.21, issue 3, 2005.

[79] **Zhang Dongxian, Zhang Haijun, Lin Xiaofeng,** Atomic force microscope in liquid with a specially designed probe for practical application, Review of Scientific Instruments, 76-053705: 1-4, 2005.

[80] **Zhang H.,** Robotic microassembly of tissue engineering scaffold, PhD Thesis, Mechanical Engineering Department, National University of Singapore, 2005.

[81] **Zhang H., Bellouard Y., Sidler T., Burdet E., Poo A.-N., Clavel R.,** A monolithic shape memory alloy microgripper for 3-D assembly of tissue engineering scaffolds, Proceedings of SPIE-Microrobotics and Microassembly III, BJ Nelson and J-M Breguet eds, 4568: 50-60, 2001.

[82] **Zhang H., Burdet E., Hutmacher D.W., Poo A.N., Bellouard Y., Clavel R., Sidler T.,** Robotic micro-assembly of scaffold/cell constructs with a shape memory alloy gripper, IEEE International Conference On Robotics And Automation, May 11-15, pp.1483 - 1488, 2002.

[83] **Zhang H., Burdet E., Poo A.N., Hutmacher D.W.,** Robotics Microassembly of tissue engineering scaffolds, IEEE Transactions on Automation Science and Engineering (in press), 2006.

[84] **Zhang H., Chollet F., Burdet E., Poo A.N., Hutmacher D.W.,** Fabrication of 3d microparts for the assembly of scaffold/cell constructs in tissue engineering, International Journal of Computational Engineering Science, pp.281 - 284, vol.4, 2003.